

On the Dynamics of Multiparticle Carroll–Schrödinger Quantum Systems

José Rojas¹ and Melvin Arias^{1,2}

¹*Instituto de Física, Universidad Autónoma de Santo Domingo, Av. Alma Mater, Santo Domingo 10105, Dominican Republic*

²*Laboratorio de Nanotecnología, Área de Ciencias Básicas y Ambientales, Instituto Tecnológico de Santo Domingo, Av. Los Próceres, Santo Domingo 10602, Dominican Republic*

December 2, 2025

Abstract

We study the dynamics of multiparticle Carroll–Schrödinger (CS) quantum systems in 1+1 dimensions, where x acts as the evolution variable and t as the configuration coordinate. We derive the N -body theory on equal- x slices as the Carrollian limit of a relativistic multi-time Klein–Gordon model, introducing temporal interactions via minimal coupling to the temporal energy operators. An x -dependent gauge transformation maps this to an equivalent description with explicit many-body potentials, illustrated by a temporal coupled-oscillator model that exhibits synchronization. Adopting a complementary spatial viewpoint with a static potential $U_{tot}(\mathbf{x})$, we show that the evolution is driven by the collective force $\sum_j \partial_{x_j} U_{tot}$; for any translation-invariant interaction (such as a regularized Coulomb potential), these internal forces cancel, rendering the collective dynamics free and highlighting Carrollian ultralocality. We also construct a coordinate duality mapping separable Schrödinger Hamiltonians to CS generators via Schwarzian derivatives. Exchange symmetry is formulated in the time domain, yielding temporal bunching for bosons and antibunching for fermions via the second-order coherence function $g^{(2)}(t, t')$. In second quantization, the contact limit yields a temporal derivative cubic–quintic nonlinear Schrödinger equation with a theoretically fixed nonlinearity coefficient $\beta = -3/16$. Finally, by coupling canonical pairs to external scalar and gauge fields, we establish an isomorphism with one-dimensional current-density functional theory, outlining a Carrollian Hohenberg–Kohn mapping and Kohn–Sham scheme.

1 Introduction

Nonrelativistic quantum mechanics on the line is usually formulated in the Schrödinger picture, where time t plays the role of evolution parameter and x is the configuration coordinate. The opposite corner of kinematical limits is the *Carroll* regime, obtained by a $c \rightarrow 0$ contraction of the Poincaré group [1]. At the level of wave equations, this limit can be implemented by the Carroll–Schrödinger (CS) equation [2, 3]

$$i\hbar c \partial_x \Psi(x, t) - \frac{1}{2mc^2} (-i\hbar \partial_t)^2 \Psi(x, t) = 0, \quad (1.1)$$

which is first order in the spatial variable x (the evolution coordinate) and second order in the temporal configuration coordinate t . This admits a unitary x -evolution on the equal- x Hilbert space $\mathcal{H} = L^2(\mathbb{R}_t, dt)$ generated by

$$H_x = \frac{\widehat{E}^2}{2mc^2}, \quad \widehat{E} := -i\hbar \partial_t, \quad (1.2)$$

self-adjoint on $H^2(\mathbb{R}_t)$ [4]. In earlier work we used this operator picture to relate Schrödinger and CS dynamics at the single-particle level, including currents, dispersion and classical limits, and to construct coordinate transformations connecting static Schrödinger potentials to time-dependent Carroll potentials, and to introduce the equal- x Hilbert space together with a proof of unitary evolution in x for the one-particle CS wave function [4].

The aim of this paper is to extend the framework to *many-body* systems and to examine, in a controlled setting, how interactions, correlations and coordinate dualities act when the roles of x and t are exchanged. We work on the equal- x Hilbert space $\mathcal{H}_N = L^2(\mathbb{R}_t^N)$ and introduce temporal interactions by minimally coupling one-body fields and two-time kernels to the temporal energy operators \widehat{E}_i . An x -dependent many-body gauge transformation produces an equivalent evolution equation in which the interaction appears as an explicit N -body potential in the time variables. For gauge potentials that are affine in x , this can be organized so that the resulting temporal potential has a prescribed form. This provides a simple mapping: starting from a standard many-body Schrödinger model one formally replaces the spatial coordinates x_i by times t_i to obtain a candidate Carrollian partner whose equal- x dynamics has the same $T+V$ structure but acts along t . As an illustration we discuss a temporal analogue of coupled harmonic oscillators, where the temporal configuration variables have the same normal-mode structure as in the spatial model.

We also adopt a complementary, purely spatial viewpoint and start from a static total potential energy $U_{tot}(\mathbf{x})$. Writing the CS evolution with U_{tot} as a shift of the temporal energy operator and performing a gauge transformation in t , we show that, in this construction, the Carrollian dynamics depends on U_{tot} through the effective force on the center of mass $\sum_j \partial_{x_j} U_{tot}(\mathbf{x})$. For coupled harmonic oscillators on a line this produces a linear-in- t drive of the collective coordinate, and, in order to illustrate the resulting dynamics, we obtain explicit Gaussian N -body solutions while showing that the multiparticle wave function’s spatial distribution and evolution are highly dependent on the boundary data, discussing their physical interpretation from the Carrollian point of view. For a regularized one-dimensional Coulomb interaction (and translation-invariant potentials generally), by contrast, the internal forces cancel in the collective direction and the transformed dynamics is free, with the interaction potential reappearing only through phases and boundary data, highlighting an important limitation of multiparticle Carroll–Schrödinger systems with purely spatial and translation-invariant internal interactions.

A second theme of the paper is a many-body generalization of the coordinate duality between the time-independent Schrödinger equation and a space-independent CS equation that was previously analyzed in the one-body setting [4]. Restricting, on the Schrödinger side, to separable N -body Hamiltonians with $\sum_i V_{\text{sch}}^{(i)}(x_i)$, we construct, for each particle, a potential-dependent reparametrization $x_i = \delta_i(t_i)$ that maps the stationary Schrödinger problem to a space-independent CS equation in the time variables with one-body Carroll potentials $V_{\text{car}}^{(i)}(t_i)$. The map is governed by Schwarzian relations for the inverse functions $\tau_i = \delta_i^{-1}$, and provides an explicit relation between families of static Schrödinger potentials and space-independent Carroll potentials acting on the temporal coordinates. This construction extends the single-particle duality of Ref. [4] to a separable many-body setting and clarifies the role of the Schrödinger energies $E_{\text{sch}}^{(i)}$ and Carroll momenta $p_0^{(i)}$ as dual labels, and we explore the Schwarzian coordinate map in an interacting example of two Schrödinger coupled harmonic oscillators.

Once the many-body generators are in place, exchange symmetry can be formulated directly in the time domain. On each equal- x slice the N -body wave function lives in $L^2(\mathbb{R}_t^N)$, and indistinguishability acts on permutations of the time labels. This leads to bosonic and fermionic sectors *in time*, defined by symmetry or antisymmetry under $t_i \leftrightarrow t_j$ at fixed x . The associated one-body density matrix and pair density quantify temporal coherence and Pauli suppression on the coincidence hyperplanes $t_i = t_j$. In this setting it is natural to introduce a second-order coherence function $g^{(2)}(t, t')$ on equal- x slices and to interpret it as a temporal analogue of Hanbury Brown–Twiss (HBT) correlations. In the noninteracting reference cases we recover temporal bunching for bosons and antibunching for fermions.

The many-body framework also supports effective field and functional descriptions. In second quantization on equal- x slices we use canonical commutation relations in the time coordinate [3] to derive a temporal nonlinear Schrödinger equation with a two-time interaction kernel. In a short-memory limit, analogous to the short-range interaction limit of a one-dimensional Lieb–Liniger gas [14, 15], where the kernel becomes local in t , the corresponding mean-field equation reduces, after simple rescalings, to a derivative cubic–quintic nonlinear Schrödinger equation (DNLS) in the time coordinate. We find that the quintic nonlinearity coefficient is geometrically fixed to $\beta = -3/16$, placing the interaction-driven temporal Carroll gas in a specific universality class of DNLS systems.

Finally, we transpose density-functional concepts to the CS setting in a static (equal- x) framework. By minimally coupling the canonical momentum P to a scalar field $\Phi(t)$ and the temporal energy E to a gauge field $U(t)$, we identify a natural mapping that renders the ground-state problem formally isomorphic to one-dimensional current-density functional theory (CDFT). Relying on this isomorphism, we introduce a universal functional $F[n, j_t]$ of the temporal density $n(t)$ and temporal current $j_t(t)$ and outline a Carrollian Kohn–Sham scheme in terms of one-time orbitals that reproduce (n, j_t) on equal- x slices.

The remainder of the paper is organized as follows. In Sec. 2 we obtain the many-body CS formalism as the limit of a relativistic multi-time Klein–Gordon system and describe a mapping to explicit temporal potentials, illustrated by a temporal coupled-oscillator model. In Sec. 3 we explore the spatial interactions viewpoint and analyze model systems of coupled harmonic oscillators and systems with Coulomb interactions, finding that translation-invariant internal spatial forces cancel in the collective Carrollian dynamics. The following section extends the single-particle coordinate duality between the time-independent Schrödinger equation and the space-independent CS equation to separable N -body systems. Section 5 discusses exchange symmetry in the time domain and

re-interprets temporal HBT correlations from a Carrollian perspective. The next section obtains a temporal nonlinear Schrödinger equation in second quantization; in the contact limit, this reduces to a derivative cubic–quintic NLSE with a geometrically determined coefficient. Finally, Section 7 outlines a proposal for a Carrollian density-functional framework. By minimally coupling the canonical momentum P to a scalar field Φ and the energy E to a gauge field U , we identify a formal isomorphism with one-dimensional current-density functional theory, which motivates a Carrollian Hohenberg–Kohn mapping and Kohn–Sham scheme. We conclude with a brief discussion of implications and limitations.

2 Many-body Carroll–Schrödinger temporal formalism

To motivate the many-body Carroll–Schrödinger (CS) generator, it is useful to start from a relativistic parent theory. We work in 1+1 dimensions and consider an N -particle Klein–Gordon field

$$\Phi(\mathbf{q}, \mathbf{t}) \equiv \Phi(q_1, \dots, q_N; t_1, \dots, t_N),$$

where each particle is described by its own space–time pair (q_i, t_i) , following Dirac’s relativistic multi-time formulation [5]. For each particle i we impose a Klein–Gordon equation in its own time coordinate t_i ,

$$\left(-\frac{1}{c^2} \partial_{t_i}^2 + \partial_{q_i}^2 + \mu^2 \right) \Phi(\mathbf{q}, \mathbf{t}) = 0, \quad \mu := \frac{mc}{\hbar}, \quad i = 1, \dots, N, \quad (2.1)$$

which is the natural many-body generalization of the one-body tachyonic Klein–Gordon equation used in Ref. [3]. Equations of the form (2.1) also fit into the multi-time-wave-function framework reviewed in Ref. [6], but here we use them only as a relativistic parent for the Carroll contraction.

In a general relativistic setting, the condition of “co-spatiality” ($q_1 = \dots = q_N = x$) is frame-dependent, much like simultaneity ($t_1 = \dots = t_N = t$). However, we are specifically interested in the Carrollian limit ($c \rightarrow 0$), where the spacetime lightcone collapses and spatial intervals become absolute while temporal intervals become relative. In this limit, the equal- x foliation becomes Carroll-invariant (since $x' \approx x$ under Carroll boosts). Therefore, we perform the reduction to equal- x slices in the reference frame where the Carroll contraction is defined, identifying it as the natural configuration space for the limiting theory.

Restricting to these equal- x slices and following the same field redefinition and Carroll scaling procedure as in Ref. [3], one finds that each pair (x, t_i) produces a one-body CS operator $\widehat{E}_i^2/(2mc^2)$ acting on the equal- x wave function $\Psi(x, \mathbf{t})$. Consistency of the x -evolution then identifies the total generator as the sum of these one-body pieces, leading to the free many-body CS equation

$$i\hbar c \partial_x \Psi(x, \mathbf{t}) = H_x^{(N)} \Psi(x, \mathbf{t}) = \sum_{i=1}^N \frac{\widehat{E}_i^2}{2mc^2} \Psi(x, \mathbf{t}), \quad (2.2)$$

with

$$H_x^{(N)} := \sum_{i=1}^N \frac{\widehat{E}_i^2}{2mc^2}, \quad \widehat{E}_i := -i\hbar \partial_{t_i}. \quad (2.3)$$

Here m is the single-particle mass; $H_x^{(N)}$ is simply the direct sum of N identical one-body Carroll generators, in exact analogy with the usual Schrödinger Hamiltonian $H_{\text{Sch}}^{(N)} = \sum_i p_i^2/(2m)$.

Although (2.1) is a multi-time system in the sense of Dirac and of Ref. [6], the resulting Carroll theory is *not* a multi-time evolution in the Schrödinger sense. After the Carroll contraction we obtain a single first-order equation in x , with t_1, \dots, t_N appearing only as configuration coordinates in the Hermitian generator $H_x^{(N)}$. There are no separate evolution equations $i\hbar\partial_{t_i}\Psi = H_i\Psi$ and therefore no compatibility conditions of the type that lead to the multi-time no-go theorems [7]. In this work we interpret (2.2) as defining a standard unitary evolution in x on equal- x slices.

On each equal- x slice the state therefore lives in the Hilbert space

$$\mathcal{H}_N := L^2(\mathbb{R}_t^N, dt), \quad \mathbf{t} = (t_1, \dots, t_N), \quad (2.4)$$

and (2.2) describes unitary x -evolution on \mathcal{H}_N . The temporal variables (t_1, \dots, t_N) play the role of configuration coordinates, so that $|\Psi(x, \mathbf{t})|^2$ is a genuine probability density in the time domain on each equal- x slice. Among the various Carrollian viewpoints, this equal- x picture is singled out by providing a linear, norm-preserving dynamics with a positive-definite density; in Sec. 3 we will contrast it with a complementary spatial perspective.

2.1 Temporal interactions

The free generator (2.3) can be generalized to include interactions in several ways. A relativistically natural option, following the dynamic-time models of Refs. [8, 9], is to introduce potentials that depend on Lorentz-invariant separations

$$\rho_{ij}^2 := c^2(t_i - t_j)^2 - (q_i - q_j)^2,$$

so that the Klein–Gordon equation acquires a nonlocal but Lorentz-invariant interaction $V(\{\rho_{ij}\})$. On equal- x slices $q_i = q_j = x$ the invariant separations reduce to purely temporal distances,

$$\rho_{ij}^2|_{q_i=q_j=x} = c^2(t_i - t_j)^2,$$

and the interaction depends only on differences of the time coordinates,

$$V(\{\rho_{ij}\})|_{q_i=q_j=x} = V(\{c|t_i - t_j|\}) \equiv V_t(\mathbf{t}).$$

Taking the Carroll limit as above then produces temporal interaction terms $V_t(\mathbf{t})$ acting on $\Psi(x, \mathbf{t})$, in addition to the free generator $H_x^{(N)}$. This provides a relativistic origin for the purely temporal many-body potentials that we will use in this section.

A complementary construction, analyzed in Sec. 3, starts instead from a static spatial potential energy $U_{\text{tot}}(\mathbf{x})$ and leads, after a gauge transformation and Carroll limit, to an effective drive governed by the collective spatial force $\sum_j \partial_{x_j} U_{\text{tot}}(\mathbf{x})$. This spatial viewpoint is useful for comparing with standard Schrödinger models, but yields rather constrained collective dynamics in strictly translation-invariant cases.

For the temporal viewpoint adopted here, it is convenient to parametrize interactions directly on \mathcal{H}_N in an *inside-the-square* form by replacing each temporal energy operator

\widehat{E}_i with a minimally coupled operator $\widehat{E}_i - A_i(x; \mathbf{t})$:

$$\mathcal{H}_{\text{in}}^{(N)}(x) := \sum_{i=1}^N \frac{1}{2mc^2} \left(\widehat{E}_i - A_i(x; \mathbf{t}) \right)^2, \quad (2.5)$$

so that the associated interacting CS equation reads

$$i\hbar c \partial_x \Psi(x, \mathbf{t}) = \mathcal{H}_{\text{in}}^{(N)}(x) \Psi(x, \mathbf{t}). \quad (2.6)$$

Here the $A_i(x; \mathbf{t})$ are real functions encoding one-body and many-body couplings in the temporal configuration coordinates. We take them of the general form

$$A_i(x; \mathbf{t}) = U(x, t_i) + \frac{1}{2} \sum_{j \neq i} \Omega(x; t_i, t_j), \quad (2.7)$$

with a one-body Carroll scalar $U(x, t)$ and a symmetric two-time kernel $\Omega(x; t, t') = \Omega(x; t', t)$.

A particularly transparent case is when the A_i arise from a single scalar phase $S(x; \mathbf{t})$, i.e.

$$A_i(x; \mathbf{t}) = \partial_{t_i} S(x; \mathbf{t}), \quad i = 1, \dots, N. \quad (2.8)$$

Defining

$$\Psi(x, \mathbf{t}) := \exp\left(\frac{i}{\hbar} S(x; \mathbf{t})\right) \Phi(x, \mathbf{t}), \quad (2.9)$$

one readily checks that Φ satisfies an *outside-the-square* CS equation

$$i\hbar c \partial_x \Phi(x, \mathbf{t}) = \left[\sum_{i=1}^N \frac{\widehat{E}_i^2}{2mc^2} + V_t(\mathbf{t}) \right] \Phi(x, \mathbf{t}), \quad (2.10)$$

provided S is chosen as

$$S(x; \mathbf{t}) := \frac{x}{c} V_t(\mathbf{t}). \quad (2.11)$$

In that case

$$A_i(x; \mathbf{t}) = \partial_{t_i} S(x; \mathbf{t}) = \frac{x}{c} \partial_{t_i} V_t(\mathbf{t}), \quad i = 1, \dots, N, \quad (2.12)$$

and the temporal potential $V_t(\mathbf{t})$ can be decomposed as

$$V_t(\mathbf{t}) = \sum_{i=1}^N U_t(t_i) + \sum_{1 \leq i < j \leq N} W_t(t_i, t_j), \quad (2.13)$$

with one-body contributions U_t and symmetric pair potentials W_t . In other words, any choice of $V_t(\mathbf{t})$ defines, via (2.11)–(2.12), an inside-the-square model (2.5) that is unitarily equivalent to the outside-the-square form (2.10). The converse is more restrictive: generic couplings of the form (2.7) need not admit such a scalar S and may not correspond to a simple local $V_t(\mathbf{t})$.

2.2 Temporal oscillators

As a concrete illustration, consider the temporal analogue of coupled harmonic oscillators. The spatial potential energy for N oscillators on a line is given by

$$V_{\text{osc}}(\mathbf{x}) = \sum_{i=1}^N \frac{1}{2} m \omega^2 x_i^2 + \frac{k_c}{2} \sum_{i<j} (x_i - x_j)^2.$$

Formally replacing $x_i \rightarrow t_i$ and introducing temporal parameters ω_t and k_t , we define the temporal potential

$$V_t^{\text{osc}}(\mathbf{t}) = \sum_{i=1}^N \frac{1}{2} m \omega_t^2 t_i^2 + \frac{k_t}{2} \sum_{i<j} (t_i - t_j)^2. \quad (2.14)$$

It is important to note that ω_t in this temporal viewpoint is not a standard temporal frequency, as time here acts as the configuration coordinate. Instead, since x is the evolution parameter, ω_t plays a role analogous to a scaled spatial wavenumber that determines the rate of oscillation as the system evolves along x , with units of acceleration. The corresponding outside-the-square CS equation is

$$i\hbar c \partial_x \Phi(x, \mathbf{t}) = \sum_{i=1}^N \frac{\widehat{E}_i^2}{2mc^2} \Phi(x, \mathbf{t}) + V_t^{\text{osc}}(\mathbf{t}) \Phi(x, \mathbf{t}), \quad (2.15)$$

which describes an N -body system of *temporal oscillators*. On each equal- x slice, the temporal coordinates t_i exhibit the same normal-mode structure as the spatial coordinates x_i do in the usual coupled-oscillator model.

To find the equivalent inside-the-square representation, we choose the scalar phase $S(x; \mathbf{t}) = \frac{x}{c} V_t^{\text{osc}}(\mathbf{t})$. The associated gauge couplings (2.12) become

$$A_i^{\text{osc}}(x; \mathbf{t}) = \frac{x}{c} \partial_{t_i} V_t^{\text{osc}}(\mathbf{t}) = \frac{x}{c} \left[(m\omega_t^2 + Nk_t) t_i - k_t \sum_{j=1}^N t_j \right], \quad (2.16)$$

which defines a Hamiltonian of the form (2.5) that is unitarily equivalent to (2.15).

Since the generator in (2.15) is quadratic in both the temporal coordinates and the temporal momentum operators \widehat{E}_i , it can be diagonalized algebraically. Letting τ_α be the temporal normal coordinates with corresponding effective frequencies ω_α , we define the temporal annihilation and creation operators

$$\hat{b}_\alpha = \sqrt{\frac{mc^2(\omega_\alpha/c)}{2\hbar}} \left(\tau_\alpha + \frac{i}{mc^2(\omega_\alpha/c)} \widehat{E}_\alpha \right), \quad \hat{b}_\alpha^\dagger = \sqrt{\frac{mc\omega_\alpha}{2\hbar}} \left(\tau_\alpha - \frac{i}{mc\omega_\alpha} \widehat{E}_\alpha \right), \quad (2.17)$$

where $\widehat{E}_\alpha = -i\hbar \partial_{\tau_\alpha}$. These operators satisfy $[\hat{b}_\alpha, \hat{b}_\beta^\dagger] = \delta_{\alpha\beta}$. The many-body Carroll generator then takes the diagonal form

$$H_{\text{total}} = \sum_{\alpha=1}^N \hbar \left(\frac{\omega_\alpha}{c} \right) \left(\hat{b}_\alpha^\dagger \hat{b}_\alpha + \frac{1}{2} \right). \quad (2.18)$$

The eigenvalues $\hbar\omega_\alpha/c$ correspond to the discrete wavenumbers for spatial propagation along x .

Physically, this model describes a mechanism for *temporal synchronization*. Just as a spatial spring enforces a fixed distance between particles, the pairwise coupling $k_t(t_i - t_j)^2$ in (2.14) imposes an energetic penalty on asynchrony. A strong coupling k_t effectively creates a “rigid body in time,” forcing the particles to arrive at any spatial slice x with fixed time delays relative to one another. In the presence of this potential, the N -body wave packet does not disperse freely along the temporal axes; instead, the interaction acts as a synchronizer, protecting the temporal coherence of the packet and ensuring that multiparticle correlations (such as the HBT signals discussed in Sec. 5) are maintained over long propagation distances.

Minimal coupling description (Inside-the-square)

Alternatively, we may describe the system via the inside-the-square representation by identifying the gauge couplings A_i directly with the temporal potential energy function. For the $N = 2$ case, we use the symmetric gauge choice

$$A_1(t_1, t_2) = \frac{1}{2}m\omega_t^2 t_1^2 + \frac{k_t}{4}(t_1 - t_2)^2, \quad (2.19)$$

$$A_2(t_1, t_2) = \frac{1}{2}m\omega_t^2 t_2^2 + \frac{k_t}{4}(t_2 - t_1)^2. \quad (2.20)$$

The Hamiltonian is defined as

$$\mathcal{H}_{\text{in}}^{(2)} = \frac{1}{2mc^2} \left[(\hat{E}_1 - A_1)^2 + (\hat{E}_2 - A_2)^2 \right]. \quad (2.21)$$

It is important to note that this inside-the-square construction is not generated by a global scalar phase S and is therefore not equivalent to the outside-the-square form (2.12). Instead, it is obtained by directly coupling an oscillator-like potential to the energy operator in the Carroll–Schrödinger equation. Since this Hamiltonian is independent of the evolution coordinate x , we seek stationary solutions of the form $\Psi(x, \mathbf{t}) = e^{-i\mathcal{E}x/\hbar c} \Psi(\mathbf{t})$, satisfying the eigenvalue equation $\mathcal{H}_{\text{in}}^{(2)} \Psi(\mathbf{t}) = \mathcal{E} \Psi(\mathbf{t})$.

To obtain the general solution, we separate the system into center-of-time $T = (t_1 + t_2)/2$ and relative time $\tau = t_1 - t_2$ coordinates. Substituting the potentials into the Hamiltonian yields

$$\mathcal{H}_{\text{in}}^{(2)} = \frac{1}{4mc^2} \left(\hat{E}_T - A_\Sigma(T, \tau) \right)^2 + \frac{1}{mc^2} \left(\hat{E}_\tau - A_\Delta(T, \tau) \right)^2, \quad (2.22)$$

where the sum and difference potentials are

$$A_\Sigma = m\omega_t^2 T^2 + \left(\frac{1}{4}m\omega_t^2 + \frac{k_t}{2} \right) \tau^2, \quad A_\Delta = \frac{1}{2}m\omega_t^2 T\tau. \quad (2.23)$$

We perform a unitary gauge transformation to decouple the interaction term A_Δ . Introducing the phase $\Lambda(T, \tau) = \frac{1}{4}m\omega_t^2 T\tau^2$, we transform the wavefunction as $\Psi = e^{i\Lambda/\hbar} \tilde{\Psi}$. This shifts the momentum operators as $\hat{E}_\tau \rightarrow \hat{E}_\tau + A_\Delta$ (canceling the coupling in the second term) and $\hat{E}_T \rightarrow \hat{E}_T + \frac{1}{4}m\omega_t^2 \tau^2$. The transformed Hamiltonian is separable

$$\tilde{\mathcal{H}} = \frac{1}{4mc^2} \left(\hat{E}_T - m\omega_t^2 T^2 - \frac{k_t}{2} \tau^2 \right)^2 + \frac{1}{mc^2} \hat{E}_\tau^2. \quad (2.24)$$

We define the operator $\hat{\mathcal{O}}_T \equiv \hat{E}_T - m\omega_t^2 T^2$. Since $\hat{\mathcal{O}}_T$ acts only on T and \hat{E}_τ^2 acts only on τ , these two operators commute. We can therefore construct the general solution as

a product of their simultaneous eigenstates, $\tilde{\Psi}(T, \tau) = f_\lambda(T)\phi_\lambda(\tau)$. The function $f_\lambda(T)$ satisfies the first-order differential equation $\hat{\mathcal{O}}_T f_\lambda = \lambda f_\lambda$, with solution

$$f_\lambda(T) = \exp \left[\frac{i}{\hbar} \left(\frac{1}{3} m \omega_t^2 T^3 + \lambda T \right) \right]. \quad (2.25)$$

Substituting the eigenvalue λ back into the Hamiltonian equation for $\phi_\lambda(\tau)$, and using the explicit differential form $\hat{E}_\tau = -i\hbar\partial_\tau$, we obtain the second-order differential equation for the relative motion

$$-\frac{\hbar^2}{mc^2} \frac{d^2\phi_\lambda}{d\tau^2} + \left[\frac{1}{4mc^2} \left(\lambda - \frac{k_t}{2} \tau^2 \right)^2 \right] \phi_\lambda(\tau) = \mathcal{E} \phi_\lambda(\tau). \quad (2.26)$$

This effective potential is a quartic well for any real λ , leading to a discrete energy spectrum and bound states. Thus, the general solution confirms that the interaction k_t enforces synchronization through temporal confinement, modulated by the continuous parameter λ . It is important to note that this inside-the-square construction is not generated by a global scalar phase S , and therefore it is not equivalent to the outside-the-square solution from the previous subsection. Rather, it arises by directly coupling an oscillator-like potential to the energy operator in our Carroll Schrödinger equation.

3 Spatial interactions viewpoint and model systems

An important question is how a multi-particle Carroll–Schrödinger (CS) system responds to *purely spatial* drives, i.e. when the interaction energy $U(\mathbf{x})$ depends only on the spatial configuration, as in standard classical and Schrödinger dynamics. Physically, this description corresponds to the Carrollian limit of a multiparticle Klein–Gordon system coupled to static spatial potentials; for internal interactions, such potentials are typically defined in the center-of-mass frame where the interaction energy acts instantaneously [8]. After examining solution behavior, continuity laws and operator structure, it is natural in 1+1 dimensions to regard the CS dynamics as an *evolution in x* with t as the configuration variable [4]. In order to compare spatial behavior on a more equal footing with standard Schrödinger systems, in this section we adopt a complementary viewpoint where we compare the usual spatial probability density $|\psi_{\text{Sch}}|^2$ with the Carroll *temporal* probability current J_t , which from a purely spatial point of view can be interpreted as an effective spatial density. It must be emphasized that in the strict Carrollian limit ($c \rightarrow 0$) space becomes absolute and causally disconnected (“frozen”) [10], meaning the physical degrees of freedom reside entirely in the temporal domain; however, we use this spatial viewpoint as a formal tool to illustrate how external potentials would act when time is treated as the evolution parameter.

The CS continuity equation (in the free case) can be written as

$$\partial_x \rho_t(x, t) + \partial_t J_t(x, t) = 0, \quad \rho_t(x, t) := |\Psi(x, t)|^2, \quad J_t(x, t) := \frac{\hbar}{mc^3} \text{Im}[\Psi^* \partial_t \Psi], \quad (3.1)$$

where the subscript t emphasizes that ρ_t and J_t are the density and current associated with the time coordinate. Exchanging the roles of density and current, the same equation can be written as

$$\partial_x J_x(x, t) + \partial_t \rho_x(x, t) = 0, \quad \rho_x(x, t) := \frac{\hbar}{mc^3} \text{Im}[\Psi^* \partial_t \Psi], \quad J_x(x, t) := |\Psi(x, t)|^2, \quad (3.2)$$

so that, in 1+1 dimensions, the dynamics can be viewed either as an x -evolution with ρ_t a positive-definite norm, or as a t -evolution with ρ_x playing the role of an effective spatial density (note that ρ_x is not positive definite, so it is not a genuine probability density, only an effective density from the dual viewpoint). In the present work, the first viewpoint is preferred (except in this section), since it provides a unitary evolution in x with a positive definite probability density ρ_t .

For these reasons, in this section we depart from the N -time configuration space of Sec. 2 and consider a more standard setting with N spatial coordinates \mathbf{x} and a single time t . From this spatial viewpoint we regard t as the evolution parameter and $\mathbf{x} = (x_1, \dots, x_N)$ as the configuration coordinates, so that the wave function is $\Psi(\mathbf{x}, t)$ rather than $\Psi(x; t_1, \dots, t_N)$. This is done solely to compare against familiar many-body Schrödinger systems in a compact way; it is not the same N -time configuration used in Sec. 2. For a configuration $\mathbf{x} = (x_1, \dots, x_N)$ and a time-independent total potential energy $U_{tot}(\mathbf{x})$, we start from the CS evolution written in the inside-the-square form

$$i\hbar c \sum_{j=1}^N \partial_{x_j} \Psi(\mathbf{x}, t) = \frac{1}{2mc^2} \left(-i\hbar \partial_t - U_{tot}(\mathbf{x}) \right)^2 \Psi(\mathbf{x}, t), \quad (3.3)$$

and define the gauge-transformed field

$$\Phi(\mathbf{x}, t) = \exp\left(-\frac{i}{\hbar} \int_{t_0}^t U_{tot}(\mathbf{x}) d\tau\right) \Psi(\mathbf{x}, t) = \exp\left(-\frac{i}{\hbar} (t - t_0) U_{tot}(\mathbf{x})\right) \Psi(\mathbf{x}, t), \quad (3.4)$$

where t_0 is a reference time. Substituting into (3.3) and dividing out the common phase gives

$$i\hbar c \sum_{j=1}^N \partial_{x_j} \Phi(\mathbf{x}, t) = -\frac{\hbar^2}{2mc^2} \partial_t^2 \Phi(\mathbf{x}, t) + c \sum_{j=1}^N \mathcal{F}_j(\mathbf{x}, t) \Phi(\mathbf{x}, t), \quad \mathcal{F}_j(\mathbf{x}, t) := \int_{t_0}^t \partial_{x_j} U_{tot}(\mathbf{x}) d\tau. \quad (3.5)$$

Because U_{tot} is independent of t , we have $\mathcal{F}_j(\mathbf{x}, t) = (t - t_0) \partial_{x_j} U_{tot}(\mathbf{x})$, and the equation simplifies to

$$i\hbar c \sum_{j=1}^N \partial_{x_j} \Phi(\mathbf{x}, t) = -\frac{\hbar^2}{2mc^2} \partial_t^2 \Phi(\mathbf{x}, t) + c(t - t_0) \sum_{j=1}^N \partial_{x_j} U_{tot}(\mathbf{x}) \Phi(\mathbf{x}, t). \quad (3.6)$$

Even for a static $U_{tot}(\mathbf{x})$ the effective drive in this linearized picture depends on both \mathbf{x} and t through the factor $c(t - t_0) \partial_{x_j} U_{tot}(\mathbf{x})$, so the dynamics is generally nonseparable and solutions are not stationary in t .

For later comparison it is useful to recall that, for the same $U_{tot}(\mathbf{x})$, the standard multi-particle Schrödinger evolution is

$$i\hbar \partial_t \psi(\mathbf{x}, t) = -\frac{\hbar^2}{2m} \sum_{j=1}^N \partial_{x_j}^2 \psi(\mathbf{x}, t) + U_{tot}(\mathbf{x}) \psi(\mathbf{x}, t), \quad (3.7)$$

with $|\psi(\mathbf{x}, t)|^2$ the spatial probability density.

3.1 Model case 1: Coupled quantum harmonic oscillators

As a first example of multi-particle Carrollian dynamics with spatial interactions, consider two coupled harmonic oscillators with total potential energy

$$U_{tot}(x_1, x_2) = \frac{1}{2} m \omega^2 (x_1^2 + x_2^2) + \frac{1}{2} k_c (x_1 - x_2)^2. \quad (3.8)$$

Substituting into (3.6) we require $\sum_j \partial_{x_j} U_{tot}$, which yields

$$\sum_{j=1}^2 \partial_{x_j} U_{tot}(x_1, x_2) = m\omega^2(x_1 + x_2). \quad (3.9)$$

Equivalently,

$$\sum_{j=1}^2 \partial_{x_j} [c(t - t_0)U_{tot}(x_1, x_2)] = m\omega^2 c(t - t_0)(x_1 + x_2), \quad (3.10)$$

The corresponding evolution equation reads

$$i\hbar c (\partial_{x_1} + \partial_{x_2})\Phi(x_1, x_2, t) = -\frac{\hbar^2}{2mc^2} \partial_t^2 \Phi(x_1, x_2, t) + c(t - t_0) m\omega^2(x_1 + x_2)\Phi(x_1, x_2, t), \quad (3.11)$$

and introducing collective and relative coordinates

$$U := x_1 + x_2, \quad V := x_1 - x_2, \quad (3.12)$$

we have $\partial_{x_1} + \partial_{x_2} = 2\partial_U$. Defining $x := U/2$ removes this factor and leads to the one-dimensional evolution

$$i\hbar c \partial_x \Phi(x, V, t) = -\frac{\hbar^2}{2mc^2} \partial_t^2 \Phi(x, V, t) + c(t - t_0) k_{\text{eff}} x \Phi(x, V, t), \quad k_{\text{eff}} := 2m\omega^2. \quad (3.13)$$

Multiplying by $2mc^2$ gives

$$i\hbar(2mc^3)\partial_x \Phi = -\hbar^2 \partial_t^2 \Phi + (2mc^3) k_{\text{eff}} x(t - t_0)\Phi, \quad (3.14)$$

Solving (3.13) via Fourier transform and the method of characteristics, we find that the resulting kernel is

$$K^{(2)}(U, V; t, t') = \sqrt{\frac{mc^3}{\pi i \hbar U}} \exp \left[-\frac{imc^3}{\hbar U} \left((t-t_0) - (t'-t_0) - \frac{k_{\text{eff}} U^3}{24mc^3} - \frac{C(V)U^2}{3c} \right)^2 - \frac{i k_{\text{eff}}^2 U^5}{320 \hbar mc^3} + \frac{i k_{\text{eff}} U^2}{4\hbar} (t-t_0) \right]. \quad (3.15)$$

with

$$C(V) = \frac{1}{\hbar} \left(\frac{m\omega^2}{4} + \frac{k_c}{2} \right) V^2. \quad (3.16)$$

The additional term proportional to $C(V)$ encodes the coupling through the integration constants of the characteristic equations.

The general solution with boundary data $\Phi_0(V, t) = \Phi(U = 0, V, t)$ is then

$$\Phi(x_1, x_2, t) = \int_{-\infty}^{\infty} dt' K^{(2)}(U, V; t, t') \Phi_0(V, t'), \quad U := x_1 + x_2, \quad V := x_1 - x_2. \quad (3.17)$$

For illustrative purposes we will choose a Gaussian initial profile

$$\Phi_0(V, t) = f(V) \frac{1}{(2\pi\sigma^2)^{1/4}} \exp \left[-\frac{(t - t_0)^2}{4\sigma^2} \right], \quad (3.18)$$

the integral remains Gaussian and yields

$$\begin{aligned} \Phi(x_1, x_2, t) = f(V) \frac{1}{(2\pi)^{1/4} \sqrt{\Sigma(U)}} \exp \left[-\frac{((t-t_0) - t_c(U, V))^2}{4\Sigma^2(U)} \right] \\ \times \exp \left\{ i \left[\chi(U) ((t-t_0) - t_c(U, V))^2 + \frac{k_{\text{eff}} U^2}{4\hbar} (t-t_0) + \varphi(U, V) \right] \right\}, \end{aligned} \quad (3.19)$$

where

$$\Sigma^2(U) = \sigma^2 + \frac{\hbar^2 U^2}{16\sigma^2 m^2 c^6}, \quad t_c(U, V) = \frac{k_{\text{eff}} U^3}{24mc^3} + \frac{C(V)U^2}{3c}, \quad \chi(U) = \frac{\hbar U}{32\sigma^2 mc^3 \Sigma^2(U)}. \quad (3.20)$$

The global phase can be chosen as

$$\varphi(U, V) = -\frac{k_{\text{eff}}^2 U^5}{320 \hbar mc^3} - \frac{1}{2} \arctan\left(\frac{\hbar U}{2\sigma^2 c}\right) - \frac{C(V)^2 U}{2mc^3}, \quad (3.21)$$

so that the normalization remains real and continuous at $U = 0$.

Returning to the original field,

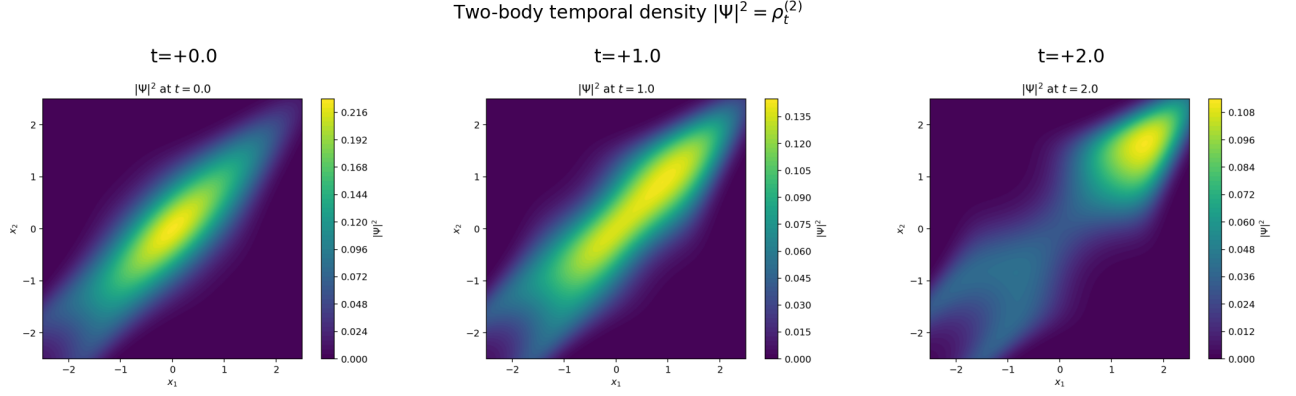
$$\Psi(x_1, x_2, t) = \exp\left(\frac{i}{\hbar}(t-t_0) U_{\text{tot}}(x_1, x_2)\right) \Phi(x_1, x_2, t), \quad |\Psi|^2 = |\Phi|^2, \quad (3.22)$$

we obtain the probability density and temporal current,

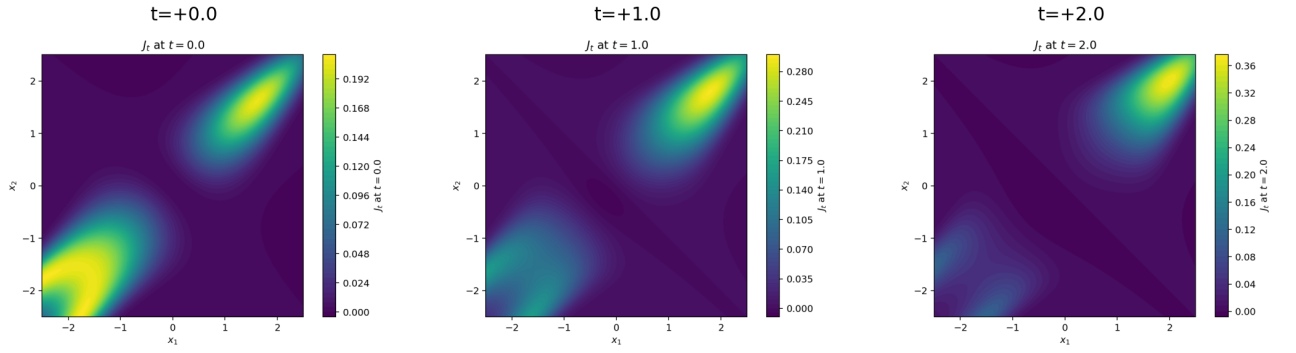
$$\rho_t^{(2)}(x_1, x_2, t) = \frac{|f(x_1 - x_2)|^2}{\sqrt{2\pi} \Sigma(x_1 + x_2)} \exp \left[-\frac{((t-t_0) - t_c(x_1 + x_2, x_1 - x_2))^2}{2\Sigma^2(x_1 + x_2)} \right], \quad (3.23)$$

$$J_t^{(2)}(x_1, x_2, t) = \rho_t^{(2)}(x_1, x_2, t) \left[\frac{\omega^2(x_1 + x_2)^2}{2c^3} + \frac{C(x_1 - x_2)}{c^2} + \frac{\hbar^2(x_1 + x_2)}{4mc^4 \sigma^2 \Sigma^2(x_1 + x_2)} ((t-t_0) - t_c(U, V)) \right], \quad (3.24)$$

describing a temporally Gaussian Carroll fluid whose width and chirp depend on the collective coordinate $U = x_1 + x_2$, while the coupling-induced drift $t_c(U, V)$ introduces a controlled temporal asymmetry along the relative coordinate.

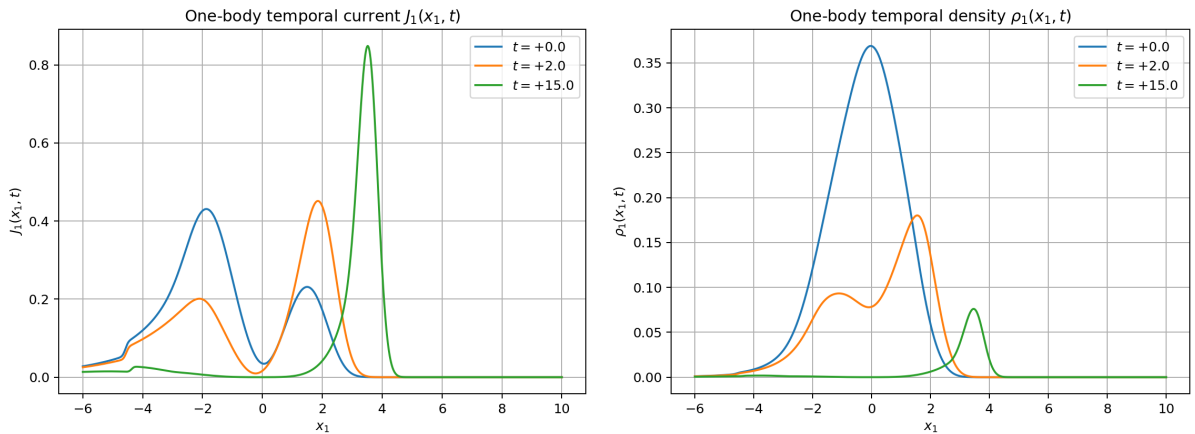


(a) Two-body temporal density $\rho_t^{(2)}(x_1, x_2, t) = |\Psi|^2$ at three times.
Two-body temporal current $J_t^{(2)}$



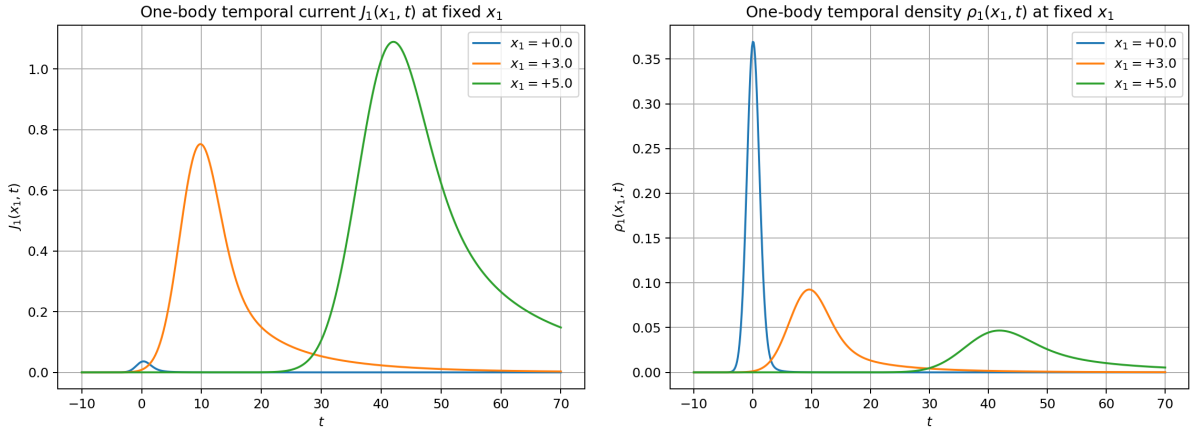
(b) Two-body temporal current $J_t^{(2)}(x_1, x_2, t)$ (which can also be interpreted as an effective Spatial density $\rho_x^{(2)}(x_1, x_2, t)$ via Eq. 3.2) at three times.

Figure 1: Carroll evolution of the two-oscillator model in the (x_1, x_2) plane.



(a) One-body temporal current $J_1(x_1, t)$ at several times t .
(b) One-body temporal density $\rho_1(x_1, t)$ at the same times.

Figure 2: Spatial profiles of the one-body observables at fixed times.



(a) One-body temporal current $J_1(x_1, t)$ at several fixed positions x_1 . (b) One-body temporal density $\rho_1(x_1, t)$ at the same positions.

Figure 3: Temporal profiles of the one-body observables at fixed x_1 .

Figures 1–3 illustrate the dynamics of the explicit Gaussian solution (3.23)–(3.24) for the parameter choice $\hbar = c = m = k_c = 1$, $\omega = 0.7$, $\sigma = 1$, $t_0 = 0$, and a normalized, even Gaussian relative profile $f(V) \propto \exp[-V^2/(2s_{\text{rel}}^2)]$ with $s_{\text{rel}} = 1$. The Carroll dynamics does not fix $f(V)$; we choose it from the spatial Schrödinger partner (relative ground state or required symmetry) and then normalize it. The genuinely Carrollian structure sits in the (U, t) sector: the dependence on the collective coordinate $U = x_1 + x_2$ and on t is governed by the kernel (3.15) through the drift time $t_c(U, V)$, while $f(V)$ and $C(V)$ control the detailed shape and parity along the relative direction.

In the two-body maps of Fig. 1, the density $\rho_t^{(2)}$ forms an elongated packet concentrated near $x_1 \simeq x_2$, with a mild skew in the V -direction coming from the $C(V)$ term. As t increases the packet drifts towards larger (x_1, x_2) and broadens along U , consistent with the temporal Gaussian being centered near $(t - t_0) \simeq t_c(U, V)$. At fixed t the probability peaks along the curve in the (x_1, x_2) plane where the drift time $t_c(U, V)$ matches the observation time. The current $J_t^{(2)}$ exhibits the same overall drift and broadening, together with the increase in magnitude as the collective packet moves to larger U , in agreement with the analytic prefactor multiplying $\rho_t^{(2)}$ in (3.24) and with the additional $C(V)/c^2$ contribution.

Figures 2 and 3 display the one-body observables obtained by integrating over x_2 . At fixed time (Fig. 2) the marginal density $\rho_1(x_1, t)$ and the current $J_1(x_1, t)$ develop single peaks that move to the right as t grows and become sharper at later times, tracking the collective drift in U and its temporal spreading. Conversely, at fixed position (Fig. 3) each x_1 sees a well-defined temporal pulse: the signal switches on, reaches a maximum near the value of t solving $t_c(U, V) \simeq t$ for the dominant values of V , and then decays as the packet moves past. These plots make explicit that, in this purely spatial model, the CS evolution is *slaved* to the boundary data on the plane $U = 0$. Once the profile $\Phi_0(V, t')$ is fixed, the bulk dynamics is obtained essentially by convolution, meaning the spatial probability density is dominantly determined by the boundary profile $f(x_1 - x_2)$. Unlike standard quantum mechanics, where interaction forces would dynamically reshape the relative wavefunction, here the evolution merely transports the initial relative configuration. This highlights the indifference of the bulk dynamics to the internal interaction potentials; the particles tend to maintain their initial relative spatial distribution rather than generating

new correlations through dynamical evolution.

N -body generalization

For N coupled harmonic oscillators on a line with nearest-neighbour coupling, the total potential energy is taken as

$$U_{tot}(\mathbf{x}) = \frac{1}{2}m\omega^2 \sum_{n=1}^N x_n^2 + \frac{1}{2}k_c \sum_{n=1}^{N-1} (x_{n+1} - x_n)^2, \quad \mathbf{x} := (x_1, \dots, x_N). \quad (3.25)$$

In the gauge-transformed outside-the-square equation (3.6), U_{tot} enters only through $\sum_j \partial_{x_j} U_{tot}$. A short computation shows that all k_c -dependent terms cancel pairwise and

$$\sum_{j=1}^N \partial_{x_j} U_{tot}(\mathbf{x}) = m\omega^2 \sum_{j=1}^N x_j. \quad (3.26)$$

Thus the coupling k_c affects the dynamics only through the relative coordinates, via the integration constants of the characteristic equations.

We introduce collective and relative coordinates

$$U := \sum_{j=1}^N x_j, \quad \mathbf{r} := (r_1, \dots, r_{N-1}), \quad r_a := x_a - x_N \quad (a = 1, \dots, N-1), \quad x := \frac{U}{N}. \quad (3.27)$$

This map $(U, \mathbf{r}) \leftrightarrow \mathbf{x}$ has constant Jacobian, spans the hyperplane orthogonal to $(1, \dots, 1)$, and any other full-rank set of $N-1$ differences is equivalent. Since $\sum_j \partial_{x_j} = N \partial_U$ and $\partial_U = \frac{1}{N} \partial_x$, we have $\sum_j \partial_{x_j} = \partial_x$, and the gauge-transformed field Φ (defined by $\Psi = e^{\frac{i}{\hbar}(t-t_0)U_{tot}} \Phi$) obeys

$$i\hbar c \partial_x \Phi(x, \mathbf{r}, t) = -\frac{\hbar^2}{2mc^2} \partial_t^2 \Phi(x, \mathbf{r}, t) + c(t-t_0) k_N x \Phi(x, \mathbf{r}, t), \quad k_N := Nm\omega^2. \quad (3.28)$$

Multiplying by $2mc^2$ gives

$$i\hbar(2mc^3) \partial_x \Phi = -\hbar^2 \partial_t^2 \Phi + (2mc^3) k_N x(t-t_0) \Phi. \quad (3.29)$$

It is convenient to separate the potential into collective and relative parts. Using (3.27) one finds

$$U_{tot}(U, \mathbf{r}) = \frac{m\omega^2}{2N} U^2 + U_{rel}(\mathbf{r}), \quad (3.30)$$

with

$$U_{rel}(\mathbf{r}) = \frac{m\omega^2}{2} \left[\sum_{a=1}^{N-1} r_a^2 - \frac{1}{N} \left(\sum_{a=1}^{N-1} r_a \right)^2 \right] + \frac{k_c}{2} \left[\sum_{n=1}^{N-2} (r_{n+1} - r_n)^2 + r_{N-1}^2 \right]. \quad (3.31)$$

For later convenience we define the (dimensionful) coupling function

$$C(\mathbf{r}) := \frac{1}{\hbar} U_{rel}(\mathbf{r}). \quad (3.32)$$

For $N=2$ one has $r_1 = x_1 - x_2 =: V$ and (3.31) reduces to $U_{rel}(V) = \left(\frac{m\omega^2}{4} + \frac{k_c}{2}\right)V^2$, so that (3.32) reproduces the two-body expression $C(V) = \left(\frac{m\omega^2}{4} + \frac{k_c}{2}\right)V^2/\hbar$ used in (3.15).

Solving (3.29) by Fourier transform in t and characteristics, one finds that the integration constants are functions of the relative coordinates \mathbf{r} , constant only with respect to U . The resulting kernel for $U \neq 0$ is

$$K_N(U, \mathbf{r}; t, t') = \sqrt{\frac{mc^3 N}{2\pi i \hbar U}} \exp \left[-\frac{imc^3 N}{2\hbar U} \left((t-t_0) - (t'-t_0) - \frac{k_N U^3}{6mc^3 N^2} - \frac{C(\mathbf{r}) U^2}{3c} \right)^2 - \frac{i k_N^2 U^5}{40 \hbar mc^3 N^3} + \frac{i k_N}{2\hbar N} U^2 (t-t_0) \right], \quad (3.33)$$

which reduces to (3.15) when $N = 2$, $U = x_1 + x_2$ and $\mathbf{r} = (V)$.

Prescribing boundary data on the hyperplane $U = 0$,

$$\Phi_0(\mathbf{r}, t) := \Phi(U = 0, \mathbf{r}, t),$$

the *general solution* can be written as

$$\Phi(\mathbf{x}, t) = \int_{-\infty}^{\infty} dt' K_N(U, \mathbf{r}; t, t') \Phi_0(\mathbf{r}, t'), \quad U = \sum_{j=1}^N x_j. \quad (3.34)$$

To explore the dynamics in closed form, we choose Gaussian temporal data at $U = 0$ with an arbitrary relative profile $f(\mathbf{r})$,

$$\Phi_0(\mathbf{r}, t) = f(\mathbf{r}) \frac{1}{(2\pi\sigma^2)^{1/4}} \exp \left[-\frac{(t-t_0)^2}{4\sigma^2} \right]. \quad (3.35)$$

Substituting (3.35) into (3.34), the integral remains Gaussian and the field is

$$\begin{aligned} \Phi(\mathbf{x}, t) = f(\mathbf{r}) \frac{1}{(2\pi)^{1/4} \sqrt{\Sigma_N(U)}} \exp \left[-\frac{((t-t_0) - t_{c,N}(U, \mathbf{r}))^2}{4\Sigma_N^2(U)} \right] \\ \times \exp \left\{ i \left[\chi_N(U) ((t-t_0) - t_{c,N}(U, \mathbf{r}))^2 + \frac{k_N}{2\hbar N} U^2 (t-t_0) + \varphi_N(U, \mathbf{r}) \right] \right\}, \end{aligned} \quad (3.36)$$

where

$$\Sigma_N^2(U) = \sigma^2 + \frac{\hbar^2 U^2}{4\sigma^2 m^2 c^6 N^2}, \quad t_{c,N}(U, \mathbf{r}) = \frac{k_N U^3}{6mc^3 N^2} + \frac{C(\mathbf{r}) U^2}{3c}, \quad \chi_N(U) = \frac{\hbar U}{8\sigma^2 mc^3 N \Sigma_N^2(U)}. \quad (3.37)$$

The function $\varphi_N(U, \mathbf{r})$ is a real, t -independent phase collecting the remaining kernel and normalization contributions; its explicit form is not needed for the densities and currents, and for $N = 2$ it reduces to the phase $\varphi(U, V)$ in (3.19).

Returning to Ψ via the gauge

$$\Psi(\mathbf{x}, t) = \exp \left(\frac{i}{\hbar} (t-t_0) U_{tot}(\mathbf{x}) \right) \Phi(\mathbf{x}, t), \quad |\Psi|^2 = |\Phi|^2, \quad (3.38)$$

we obtain the N -body temporal density

$$\rho_t^{(N)}(\mathbf{x}, t) = |\Psi|^2 = \frac{|f(\mathbf{r})|^2}{\sqrt{2\pi} \Sigma_N(U)} \exp \left[-\frac{((t-t_0) - t_{c,N}(U, \mathbf{r}))^2}{2\Sigma_N^2(U)} \right], \quad (3.39)$$

and the corresponding gauge-invariant temporal current

$$J_t^{(N)}(\mathbf{x}, t) = \rho_t^{(N)}(\mathbf{x}, t) \left[\frac{\omega^2 U^2}{Nc^3} + \frac{C(\mathbf{r})}{c^2} + \frac{\hbar^2}{2mc^4 \sigma^2 N} \frac{U}{\Sigma_N^2(U)} \left((t-t_0) - t_{c,N}(U, \mathbf{r}) \right) \right], \quad U = \sum_{j=1}^N x_j. \quad (3.40)$$

For $N = 2$ and $\mathbf{r} = (V)$, the expressions (3.36)–(3.40) reduce to the two-body formulas (3.19), (3.23) and (3.24), with $C(\mathbf{r}) \rightarrow C(V)$.

3.2 Model case 2: Coulombic interactions

For N particles on a line, consider the (regularized) Coulomb potential

$$U_C(\mathbf{x}) = - \sum_{1 \leq j < k \leq N} \frac{k_e q_j q_k}{|x_j - x_k|}, \quad \partial_{x_j} U_C(\mathbf{x}) = \sum_{k \neq j} \frac{k_e q_j q_k}{|x_j - x_k|^3} (x_j - x_k). \quad (3.41)$$

We tacitly assume a short-distance regularization so that all derivatives are bounded at $x_j = x_k$.

In the gauge-transformed outside-the-square equation (3.6), the Coulomb potential enters only through the combination $\sum_j \partial_{x_j} U_{tot}(\mathbf{x})$. For the purely Coulombic case $U_{tot} = U_C$, this sum vanishes identically. Indeed,

$$\sum_{j=1}^N \partial_{x_j} U_C(\mathbf{x}) = - \sum_{1 \leq j < k \leq N} k_e q_j q_k \left(\partial_{x_j} \frac{1}{|x_j - x_k|} + \partial_{x_k} \frac{1}{|x_j - x_k|} \right). \quad (3.42)$$

each pair (j, k) contributes zero in the sum,

$$\partial_{x_j} \frac{1}{|x_j - x_k|} + \partial_{x_k} \frac{1}{|x_j - x_k|} = 0 \quad \implies \quad \sum_{j=1}^N \partial_{x_j} U_C(\mathbf{x}) = 0. \quad (3.43)$$

This is Newton's third law in disguise: internal Coulomb forces add up to zero in the center-of-mass direction. As a result, for purely Coulombic interactions the gauge-transformed Carroll-Schrödinger equation (3.6) reduces to the *free* Carroll-Schrödinger equation

$$i\hbar c \sum_{j=1}^N \partial_{x_j} \Phi(\mathbf{x}, t) = - \frac{\hbar^2}{2mc^2} \partial_t^2 \Phi(\mathbf{x}, t), \quad (3.44)$$

while the original field is obtained by the t -dependent gauge

$$\Psi(\mathbf{x}, t) = \exp\left(\frac{i}{\hbar}(t - t_0) U_C(\mathbf{x})\right) \Phi(\mathbf{x}, t), \quad |\Psi|^2 = |\Phi|^2. \quad (3.45)$$

Thus, Coulomb interactions enter the collective evolution through the phase and through the choice of boundary data, while the bulk kernel governing the center-of-mass direction coincides with that of a free system.

This model highlights an important limitation of multi-particle Carroll-Schrödinger systems with purely spatial, translation-invariant internal interactions. Whenever $U_{tot}(\mathbf{x})$ is invariant under global translations, the internal forces cancel in the collective drive $\sum_j \partial_{x_j} U_{tot}(\mathbf{x})$ and do not generate additional collective driving terms beyond those already present in the free case. As a result, once the boundary/initial data on the collective

hyperplane are fixed, the subsequent collective evolution is governed by the same kernel as in the free system, and the detailed relative-coordinate dynamics is not directly resolved by the collective CS equation. Physically, this behavior is a direct manifestation of Carrollian ultralocality. In the limit $c \rightarrow 0$, light cones collapse and spatial points become causally disconnected, implying that spatial gradients are suppressed and interactions become ultralocal in space [10, 11]. Consequently, a purely spatial potential cannot mediate propagation between separated points in the way it does in non-relativistic mechanics; the “freezing” of the relative spatial configuration is thus not a defect of the model, but a feature of the underlying Carrollian geometry.

4 From the many-body time-independent Schrödinger equation to a space-independent many-body Carroll–Schrödinger equation

In our previous one-body analysis [4] we showed that, for a space-independent Carroll potential $V_{\text{car}}(t)$, the space-independent Carroll–Schrödinger equation can be related to a time-independent Schrödinger problem by a reparametrization $x = \delta(t)$, with the two potentials linked through a Schwarzian relation. Here we extend this construction to a simple but useful many-body setting, namely an N -particle time-independent Schrödinger equation with a *separable* potential. This suffices to build a space-independent many-body Carroll system on $L^2(\mathbb{R}_t^N)$, and provides a convenient bridge between stationary Schrödinger models and the temporal Carroll framework developed in Sec. 5.

Consider N identical particles of mass m on the line with a separable static potential,

$$\left[-\frac{\hbar^2}{2m} \sum_{i=1}^N \partial_{x_i}^2 + \sum_{i=1}^N V_{\text{sch}}^{(i)}(x_i) \right] \Psi_{\text{sch}}(\mathbf{x}) = E_{\text{sch}} \Psi_{\text{sch}}(\mathbf{x}), \quad \mathbf{x} = (x_1, \dots, x_N), \quad (4.1)$$

where $V_{\text{sch}}^{(i)}$ are one-body potentials. (More general interacting N -body non-separable potentials require genuinely multivariable reparametrizations and will not be considered here.) In the separable case, we may seek stationary product states of the form

$$\Psi_{\text{sch}}(\mathbf{x}) = \prod_{i=1}^N \psi_i(x_i), \quad E_{\text{sch}} = \sum_{i=1}^N E_{\text{sch}}^{(i)}, \quad (4.2)$$

with each factor solving a one-dimensional time-independent Schrödinger equation

$$-\frac{\hbar^2}{2m} \psi_i''(x_i) + V_{\text{sch}}^{(i)}(x_i) \psi_i(x_i) = E_{\text{sch}}^{(i)} \psi_i(x_i), \quad i = 1, \dots, N. \quad (4.3)$$

For indistinguishable particles, bosonic or fermionic symmetry can be enforced by symmetrizing or antisymmetrizing the products (4.2); the mapping constructed below acts coordinate-wise and may be extended to these symmetrized sectors.

On the Carroll side we consider space-independent many-body generators built from N temporal configuration variables $\mathbf{t} = (t_1, \dots, t_N)$ on equal- x slices, with one-body Carroll potentials $V_{\text{car}}^{(i)}(t_i)$,

$$\left[\sum_{i=1}^N \frac{1}{2mc^2} \left(-i\hbar \partial_{t_i} - V_{\text{car}}^{(i)}(t_i) \right)^2 - cP_0 \right] \Phi(\mathbf{t}) = 0, \quad (4.4)$$

where P_0 is a constant (the total Carroll momentum along the evolution coordinate x). Just as in the one-body case, it is useful to parametrize P_0 in terms of positive “energy labels” $E_0^{(i)}$,

$$cp_0^{(i)} = \frac{[E_0^{(i)}]^2}{2mc^2}, \quad P_0 = \sum_{i=1}^N p_0^{(i)}, \quad (4.5)$$

so that the multi-time equation (4.4) admits a separated solution of the form

$$\Phi(\mathbf{t}) = \prod_{i=1}^N \phi_i(t_i), \quad \frac{1}{2mc^2} \left(-i\hbar \frac{d}{dt_i} - V_{\text{car}}^{(i)}(t_i) \right)^2 \phi_i(t_i) - cp_0^{(i)} \phi_i(t_i) = 0. \quad (4.6)$$

As in the one-body discussion, the defining separation parameters are the Carroll momenta $p_0^{(i)}$; the corresponding labels $E_0^{(i)} = \pm \sqrt{2mc^3 p_0^{(i)}}$ are two-to-one functions of $p_0^{(i)}$.

The goal of this section is to exhibit, for each i , a coordinate reparametrization $x_i = \delta_i(t_i)$ relating (4.3) and (4.6), and then to assemble these one-dimensional maps into a many-body correspondence between (4.1) and (4.4).

4.1 Coordinate reparametrization and one-body mapping

We now recall the one-body construction of [4], adapted to the i th coordinate. Let

$$x_i = \delta_i(t_i), \quad \psi_i(x_i) \longrightarrow \phi_i(t_i) := \psi_i(\delta_i(t_i)), \quad (4.7)$$

with δ_i a smooth, monotone reparametrization. Writing $\dot{\delta}_i = d\delta_i/dt_i$, a direct application of the chain rule gives

$$\partial_{x_i} \psi_i = \frac{1}{\dot{\delta}_i} \partial_{t_i} \phi_i, \quad \partial_{x_i}^2 \psi_i = \frac{1}{\dot{\delta}_i^2} \partial_{t_i}^2 \phi_i - \frac{\ddot{\delta}_i}{\dot{\delta}_i^3} \partial_{t_i} \phi_i. \quad (4.8)$$

Substituting into the time-independent Schrödinger equation (4.3) yields, after a simple rearrangement,

$$-\frac{\hbar^2}{2m} \left[\frac{\ddot{\phi}_i}{\dot{\delta}_i^2} - \frac{\dot{\phi}_i \ddot{\delta}_i}{\dot{\delta}_i^3} \right] + V_{\text{sch}}^{(i)}(\delta_i(t_i)) \phi_i(t_i) - E_{\text{sch}}^{(i)} \phi_i(t_i) = 0. \quad (4.9)$$

Multiplying (4.9) by $\dot{\delta}_i^2/c^2$ and comparing with the expanded space-independent Carroll equation (4.6),

$$-\frac{\hbar^2}{2mc^2} \ddot{\phi}_i + \frac{i\hbar V_{\text{car}}^{(i)}(t_i)}{mc^2} \dot{\phi}_i + \left[\frac{i\hbar}{2mc^2} \frac{dV_{\text{car}}^{(i)}}{dt_i} + \frac{(V_{\text{car}}^{(i)}(t_i))^2}{2mc^2} - cp_0^{(i)} \right] \phi_i(t_i) = 0, \quad (4.10)$$

we obtain the one-dimensional relations

$$\frac{\ddot{\delta}_i}{\dot{\delta}_i} = \frac{2i}{\hbar} V_{\text{car}}^{(i)}(t_i), \quad V_{\text{sch}}^{(i)}(\delta_i(t_i)) = E_{\text{sch}}^{(i)} + \frac{1}{2m \dot{\delta}_i^2} \left[i\hbar \frac{dV_{\text{car}}^{(i)}}{dt_i} + (V_{\text{car}}^{(i)}(t_i))^2 - (E_0^{(i)})^2 \right]. \quad (4.11)$$

The first equation integrates to

$$\delta_i(t_i) = C_1^{(i)} + C_0^{(i)} \int^{t_i} \exp\left(\frac{2i}{\hbar} \int^{t'} V_{\text{car}}^{(i)}(s) ds\right) dt', \quad (4.12)$$

with any lower limits absorbed into the constants $C_0^{(i)}, C_1^{(i)}$. Eliminating $V_{\text{car}}^{(i)}$ from (4.11) via $V_{\text{car}}^{(i)} = -\frac{i\hbar}{2} \ddot{\delta}_i / \dot{\delta}_i$ leads to the Schwarzian form

$$V_{\text{sch}}^{(i)}(\delta_i(t_i)) - E_{\text{sch}}^{(i)} = \frac{\hbar^2}{4m} \frac{\{\delta_i, t_i\}}{\dot{\delta}_i^2} - \frac{(E_0^{(i)})^2}{2m} \frac{1}{\dot{\delta}_i^2}, \quad \{\delta_i, t_i\} := \frac{\delta_i'''}{\delta_i'} - \frac{3}{2} \left(\frac{\delta_i''}{\delta_i'} \right)^2. \quad (4.13)$$

Writing $\tau_i(x_i) := \delta_i^{-1}(x_i)$ and using the inversion identities $(\{\delta_i, t_i\} / \dot{\delta}_i^2)|_{t_i=\tau_i(x_i)} = -\{\tau_i, x_i\}$, $(1/\dot{\delta}_i^2)|_{t_i=\tau_i(x_i)} = \tau_i'(x_i)^2$, we arrive at the inverse equation

$$\boxed{\{\tau_i, x_i\} + \frac{2(E_0^{(i)})^2}{\hbar^2} \tau_i'(x_i)^2 = -\frac{4m}{\hbar^2} (V_{\text{sch}}^{(i)}(x_i) - E_{\text{sch}}^{(i)})}, \quad i = 1, \dots, N. \quad (4.14)$$

Equation (4.14) is the many-body analogue, coordinate by coordinate, of the one-body inverse relation [4]. As before, it can be linearized by using the Schwarzian chain rule. For each i we pick a function f_i with constant Schwarzian $\{f_i, u\} = 2(E_0^{(i)}/\hbar)^2$, for instance $f_i(u) = \tan(\frac{E_0^{(i)}}{\hbar}u)$, and define

$$\sigma_i(x_i) := f_i(\tau_i(x_i)) = \tan\left(\frac{E_0^{(i)}}{\hbar} \tau_i(x_i)\right), \quad (4.15)$$

so that $\{\sigma_i, x_i\} = \{\tau_i, x_i\} + \frac{2(E_0^{(i)})^2}{\hbar^2} \tau_i'^2$. Then (4.14) reduces to the pure Schwarzian equation

$$\boxed{\{\sigma_i, x_i\} = -\frac{4m}{\hbar^2} (V_{\text{sch}}^{(i)}(x_i) - E_{\text{sch}}^{(i)})}, \quad i = 1, \dots, N. \quad (4.16)$$

A standard construction shows that if $y_1^{(i)}, y_2^{(i)}$ form a fundamental system of the linear ODE

$$y''(x_i) + q_i(x_i) y(x_i) = 0, \quad q_i(x_i) := \frac{2m}{\hbar^2} (V_{\text{sch}}^{(i)}(x_i) - E_{\text{sch}}^{(i)}), \quad (4.17)$$

then $\sigma_i(x_i) = y_1^{(i)}(x_i)/y_2^{(i)}(x_i)$ satisfies $\{\sigma_i, x_i\} = -2q_i(x_i)$ and hence (4.16). Thus, on any interval where $y_2^{(i)}$ has no zeros and τ_i is monotone,

$$\sigma_i(x_i) = \frac{y_1^{(i)}(x_i)}{y_2^{(i)}(x_i)}, \quad \tau_i(x_i) = \frac{\hbar}{E_0^{(i)}} \arctan(\sigma_i(x_i)), \quad \boxed{\delta_i(t_i) = \tau_i^{-1}(t_i)}. \quad (4.18)$$

Substituting (4.18) into (4.13) and (4.11) reproduces the original $V_{\text{sch}}^{(i)}(x_i)$ and determines the associated Carroll potential $V_{\text{car}}^{(i)}(t_i)$ via $V_{\text{car}}^{(i)} = -\frac{i\hbar}{2} \ddot{\delta}_i / \dot{\delta}_i$.

4.2 A preliminary interacting example: two coupled harmonic oscillators

As an illustration of how an interacting static potential can be incorporated into this framework, we consider the two-body coupled harmonic oscillator potential

$$V_{\text{sch}}^{(2)}(x_1, x_2) = \frac{1}{2} m \omega^2 (x_1^2 + x_2^2) + \frac{1}{2} k_c (x_1 - x_2)^2. \quad (4.19)$$

By introducing center-of-mass and relative coordinates, $X = (x_1 + x_2)/2$ and $\xi = x_1 - x_2$, the kinetic energy separates into terms with total mass $M = 2m$ and reduced mass $\mu = m/2$. The potential energy diagonalizes similarly,

$$V_{\text{sch}}^{(2)}(X, \xi) = \frac{1}{2}M\Omega_X^2 X^2 + \frac{1}{2}\mu\Omega_\xi^2 \xi^2, \quad (4.20)$$

with effective frequencies given by $\Omega_X = \omega$ and $\Omega_\xi = \sqrt{\omega^2 + 2k_c/m}$.

The stationary problem thus factorizes into two independent one-dimensional channels. We can therefore apply the coordinate duality defined by Eq. (4.16) independently to each mode. This yields two reparametrization functions, $X = \delta_X(t_X)$ and $\xi = \delta_\xi(t_\xi)$, determined by the Schwarzian equations for the effective potentials $V_{\text{sch}}^{(X)} = \frac{1}{2}M\Omega_X^2 X^2$ and $V_{\text{sch}}^{(\xi)} = \frac{1}{2}\mu\Omega_\xi^2 \xi^2$.

To recover the relationship between the physical coordinates and the particle times, we invert the spatial linear transformation and substitute the temporal normal modes $t_X = (t_1 + t_2)/2$ and $t_\xi = t_1 - t_2$. This yields the mixed map

$$x_1 = \delta_X\left(\frac{t_1 + t_2}{2}\right) + \frac{1}{2}\delta_\xi(t_1 - t_2), \quad (4.21)$$

$$x_2 = \delta_X\left(\frac{t_1 + t_2}{2}\right) - \frac{1}{2}\delta_\xi(t_1 - t_2). \quad (4.22)$$

Finally, the resulting Carroll generator is defined by the sum of the effective potentials evaluated at these temporal arguments

$$V_{\text{car}}^{(2)}(t_1, t_2) = V_{\text{car}}^{(X)}\left(\frac{t_1 + t_2}{2}\right) + V_{\text{car}}^{(\xi)}(t_1 - t_2). \quad (4.23)$$

This example demonstrates that spatial entanglement arising from potential coupling in the Schrödinger picture maps to a mixing of temporal coordinates in the Carrollian picture, mediated by the mode-dependent reparametrizations.

5 Exchange symmetry in the time domain and Hanbury Brown–Twiss correlations

5.1 Exchange symmetry of multiparticle CS equation

On each equal- x slice the N -body state is

$$\Psi(x; \mathbf{t}) \in L^2(\mathbb{R}_{\mathbf{t}}^N), \quad \mathbf{t} = (t_1, \dots, t_N),$$

as in Ref. [4]. Since the Carroll–Schrödinger (CS) equation evolves in x and treats t as the configuration coordinate, exchange acts on the time labels t_1, \dots, t_N within each equal- x slice, just as it acts on spatial labels on equal-time slices in standard Schrödinger theory with stationary fields. For indistinguishable particles, physical probabilities must be invariant under any permutation $\pi \in S_N$,

$$\|\Psi(x; \mathbf{t})\|^2 = \int dt |\Psi(x; \mathbf{t})|^2 = \int dt |\Psi(x; t_{\pi(1)}, \dots, t_{\pi(N)})|^2,$$

so there is a unitary representation U_π acting as

$$(U_\pi \Psi)(x; \mathbf{t}) = \Psi(x; t_{\pi(1)}, \dots, t_{\pi(N)}).$$

If the statistics sector is one-dimensional under U_π , then $U_\pi \Psi = \chi(\pi) \Psi$ with $|\chi(\pi)| = 1$. Since transpositions τ_{ij} generate S_N and $\tau_{ij}^2 = 1$, one has

$$\chi(\tau_{ij})^2 = 1 \implies \chi(\tau_{ij}) \in \{+1, -1\},$$

which extends to a character of all S_N . This leaves the two sectors

$$\Psi_B(x; \mathbf{t}) = +\Psi_B(x; t_{\pi(1)}, \dots, t_{\pi(N)}), \quad \Psi_F(x; \mathbf{t}) = -\Psi_F(x; t_{\pi(1)}, \dots, t_{\pi(N)}), \quad \forall \pi \in S_N.$$

These are the bosonic and fermionic sectors *in the time domain*: “fermionic in time” means antisymmetry under $t_i \leftrightarrow t_j$ at fixed x , the direct analogue of exchange acting on spatial labels at fixed time.

For later use we introduce the shorthand

$$\mathbf{t}_{a:b} := (t_a, t_{a+1}, \dots, t_b), \quad d\mathbf{t}_{a:b} := dt_a dt_{a+1} \cdots dt_b.$$

With this notation, the equal- x pair density

$$n^{(2)}(t, t') = N(N-1) \int_{\mathbb{R}^{N-2}} |\Psi(x; t, t', \mathbf{t}_{3:N})|^2 d\mathbf{t}_{3:N} \quad (5.1)$$

is the reduced density for finding one time at t and another at t' on the slice. For a fermionic-in-time state, antisymmetry under exchanging any two time labels enforces nodes on the coincidence hyperplanes $t = t'$, i.e.

$$\Psi(x; \dots, t, \dots, t, \dots) = 0,$$

and therefore $n^{(2)}(t, t) = 0$. This is Pauli suppression *in time* (temporal antibunching).

To quantify temporal coherence on a slice we introduce the equal- x one-body reduced density matrix (1RDM),

$$\gamma(t, t') = N \int_{\mathbb{R}^{N-1}} \Psi(x; t, \mathbf{t}_{2:N}) \Psi(x; t', \mathbf{t}_{2:N})^* d\mathbf{t}_{2:N}, \quad n(t) = \gamma(t, t), \quad (5.2)$$

whose diagonal $n(t)$ is the one-body temporal density. The kernel γ is Hermitian and positive semidefinite, with $\text{Tr} \gamma = \int n(t) dt = N$.

5.2 Hanbury Brown–Twiss correlations

The pair density and 1RDM also encode an equal- x analogue of Hanbury Brown–Twiss (HBT) correlations [12, 13]. On a given slice we interpret $n(t) dt$ as the single-particle detection density in the interval $(t, t + dt)$, while $n^{(2)}(t, t') dt dt'$ is the joint detection density in $(t, t + dt) \times (t', t' + dt')$. This motivates the normalized temporal second-order coherence function

$$g^{(2)}(t, t') := \frac{n^{(2)}(t, t')}{n(t) n(t')}. \quad (5.3)$$

It is convenient to express $g^{(2)}$ in terms of the 1RDM. Defining the normalized first-order coherence

$$g^{(1)}(t, t') := \frac{\gamma(t, t')}{\sqrt{n(t) n(t')}}, \quad (5.4)$$

one finds, for the noninteracting Bose and Fermi reference states built from orthonormal time-orbitals, the standard Wick factorization relations

$$n_{\text{F}}^{(2)}(t, t') = n(t) n(t') - |\gamma(t, t')|^2, \quad (5.5)$$

$$n_{\text{B}}^{(2)}(t, t') = n(t) n(t') + |\gamma(t, t')|^2, \quad (5.6)$$

and therefore

$$g_{\text{F}}^{(2)}(t, t') = 1 - \frac{|\gamma(t, t')|^2}{n(t) n(t')} = 1 - |g^{(1)}(t, t')|^2, \quad (5.7)$$

$$g_{\text{B}}^{(2)}(t, t') = 1 + \frac{|\gamma(t, t')|^2}{n(t) n(t')} = 1 + |g^{(1)}(t, t')|^2. \quad (5.8)$$

On the coincidence line $t' = t$, using $\gamma(t, t) = n(t)$, we obtain

$$g_{\text{F}}^{(2)}(t, t) = 0, \quad g_{\text{B}}^{(2)}(t, t) = 1 + \frac{|\gamma(t, t)|^2}{n(t)^2} = 2, \quad (5.9)$$

in agreement with the Pauli suppression in time inferred from Eq. (5.1). Ideal Carroll fermions in time exhibit perfect temporal antibunching, while ideal Carroll bosons display temporal bunching with $g^{(2)}(t, t) = 2$ on each equal- x slice. Away from the coincidence line, the modulus of $g^{(1)}$ in Eqs. (5.7)–(5.8) measures the temporal coherence length of the Carroll gas.

These expressions suggest a Carrollian HBT protocol. One prepares the system in a fixed equal- x state $\Psi(x_0; \mathbf{t})$, lets it propagate according to CS dynamics, and places a detector at a downstream position x . On each run the detector records a list of arrival times $\{t_1^{(r)}, \dots, t_{M_r}^{(r)}\}$, from which empirical estimates of $n(t)$, $n^{(2)}(t, t')$, and hence $g^{(2)}(t, t')$ can be constructed. In the noninteracting limit the outcomes are governed by Eqs. (5.7)–(5.9); temporal interactions introduced later deform γ and $n^{(2)}$, thus modifying the shape of $g^{(2)}(t, t')$. Temporal HBT measurements at fixed x then provide an operational probe of many-body structure and statistics *in the time domain* for Carrollian quantum systems.

6 From many-body CS to a temporal DNLS

We work on equal- x slices in second quantization. The field operators satisfy the canonical equal- x relations [3]

$$[\hat{\psi}(x, t), \hat{\psi}^\dagger(x, t')] = \frac{1}{c} \delta(t - t'), \quad [\hat{\psi}(x, t), \hat{\psi}(x, t')] = [\hat{\psi}^\dagger(x, t), \hat{\psi}^\dagger(x, t')] = 0, \quad (6.1)$$

so that the Hamiltonian $\hat{H}(x)$ generates x -evolution in the Heisenberg picture via

$$i\hbar c \frac{d\hat{\mathcal{O}}}{dx} = [\hat{\mathcal{O}}, \hat{H}(x)] + i\hbar c \left(\frac{\partial \hat{\mathcal{O}}}{\partial x}\right)_{\text{explicit}}, \quad \text{with} \quad \boxed{\hat{H}(x) = c \hat{P}(x)} \quad (6.2)$$

where $\hat{P}(x)$ is the x -momentum generator on the equal- x slice. For historical reasons we use the “energy” generator $\hat{H}(x) = c \hat{P}(x)$, rather than $\hat{P}(x)$ itself, as the basic generator of x -evolution [4]. Defining the Hamiltonian as

$$\begin{aligned} \hat{H}(x) &= \int c dt : \hat{\psi}^\dagger(x, t) \frac{1}{2mc^2} \left(\hat{E} - \hat{\mathcal{A}}(x, t) \right)^2 \hat{\psi}(x, t) :, \\ \hat{E} &= -i\hbar \partial_t, \quad \hat{n}(x, t) = \hat{\psi}^\dagger(x, t) \hat{\psi}(x, t), \end{aligned} \quad (6.3)$$

where colons indicate normal ordering and the temporal “gauge field” $\hat{\mathcal{A}}(x, t)$ encodes both one-body and two-body interactions,

$$\hat{\mathcal{A}}(x, t) := U(x, t) + c \int dt' w(x; t, t') \hat{n}(x, t'). \quad (6.4)$$

Here $U(x, t)$ is a real external temporal potential and $w(x; t, t') = w(x; t', t)$ is a real symmetric two-time kernel representing short-range temporal interactions.

The Heisenberg equation for the temporal field operator follows from (6.2) by choosing $\hat{\mathcal{O}} = \hat{\psi}(x, t)$,

$$i\hbar c \partial_x \hat{\psi}(x, t) = [\hat{\psi}(x, t), \hat{H}(x)]. \quad (6.5)$$

Because $\hat{H}(x)$ is quadratic in the shifted energy operator $\hat{E} - \hat{\mathcal{A}}$ and $\hat{\mathcal{A}}$ itself depends on the density \hat{n} , evaluating the commutator requires repeated use of the canonical relations (6.1). In particular,

$$[\hat{\psi}(x, t), \hat{n}(x, t')] = \frac{1}{c} \delta(t-t') \hat{\psi}(x, t), \quad (6.6)$$

To define a contact-in-time limit, we appeal to the physical constraints of the Carrollian regime. In the $c \rightarrow 0$ limit, finite propagation speeds are suppressed, and interactions tend toward ultralocality. We assume that the collision duration (or “memory time”) of the interaction kernel is much shorter than the characteristic temporal coherence scale of the macroscopic envelope (this is the temporal analogue of the Lieb-Liniger potential [14]). Under this short-memory approximation, the kernel acts instantaneously

$$w(x; t, t') \longrightarrow g(x) \delta(t - t'). \quad (6.7)$$

This is the temporal analogue of the standard Fermi pseudopotential in spatial cold atom physics. In this limit, the temporal gauge field becomes local in t at the operator level

$$\hat{\mathcal{A}}(x, t) = U(x, t) + c g(x) \hat{n}(x, t), \quad (6.8)$$

with $g(x)$ representing the contact interaction strength. Substituting (6.8) into (6.3) and using (6.1) and (6.6), the Heisenberg equation (6.5) yields the operator evolution equation

$$\begin{aligned} i\hbar c \partial_x \hat{\psi}(x, t) = & -\frac{\hbar^2}{2mc^2} \partial_t^2 \hat{\psi}(x, t) + \frac{i\hbar}{2mc^2} (\partial_t U(x, t)) \hat{\psi}(x, t) + \frac{i\hbar}{mc^2} U(x, t) \partial_t \hat{\psi}(x, t) + \\ & \frac{2i\hbar g(x)}{mc} \hat{n}(x, t) \partial_t \hat{\psi}(x, t) + \frac{1}{2mc^2} \left[U(x, t)^2 + 4c g(x) U(x, t) \hat{n}(x, t) + 3c^2 g(x)^2 \hat{n}(x, t)^2 \right] \hat{\psi}(x, t), \end{aligned} \quad (6.9)$$

Now taking the mean-field limit of the operator evolution equation

$$\hat{\psi}(x, t) \rightarrow \phi(x, t), \quad \hat{n}(x, t) \rightarrow |\phi(x, t)|^2, \quad \hat{n}(x, t)^2 \rightarrow |\phi(x, t)|^4, \quad (6.10)$$

we arrive at the nonlinear evolution equation

$$\begin{aligned} i\hbar c \partial_x \phi(x, t) = & -\frac{\hbar^2}{2mc^2} \partial_t^2 \phi(x, t) + \frac{i\hbar}{2mc^2} (\partial_t U(x, t)) \phi(x, t) + \frac{i\hbar}{mc^2} U(x, t) \partial_t \phi(x, t) + \\ & \frac{2i\hbar g(x)}{mc} |\phi(x, t)|^2 \partial_t \phi(x, t) + \frac{1}{2mc^2} \left[U(x, t)^2 + 4c g(x) U(x, t) |\phi(x, t)|^2 + 3c^2 g(x)^2 |\phi(x, t)|^4 \right] \phi(x, t), \end{aligned} \quad (6.11)$$

In the simplest case of a purely interaction-driven temporal gas, $U(x, t) = 0$, the mean-field equation (6.11) reduces to

$$i\hbar c \partial_x \phi(x, t) = -\frac{\hbar^2}{2mc^2} \partial_t^2 \phi(x, t) + \frac{2i\hbar g(x)}{mc} |\phi(x, t)|^2 \partial_t \phi(x, t) + \frac{3g(x)^2}{2m} |\phi(x, t)|^4 \phi(x, t), \quad (6.12)$$

with $|\phi|^2 = |\phi(x, t)|^2$. For constant interaction strength $g(x) = g_0$, this equation is structurally similar to the family of cubic–quintic derivative nonlinear Schrödinger (DNLS) equations appearing in nonlinear optics and plasma physics [16–18].

To determine the specific coefficients, we bring the physical evolution equation (6.12) into a dimensionless form using the rescaling $x = LX$, $t = \tau T$, and $\phi = \mathcal{A}\psi$, where τ is the characteristic pulse width. The dynamical scales are fixed by balancing the kinetic and nonlinear terms, yielding the characteristic length $L = 2mc^3\tau^2/\hbar$ and field amplitude $\mathcal{A} = \sqrt{\hbar/(4g_0c\tau)}$. Substituting these scales reveals that the quintic coefficient β is strictly determined by the minimal coupling structure of the theory. The resulting dimensionless equation is:

$$i\partial_X \psi + \partial_T^2 \psi - i|\psi|^2 \partial_T \psi - \frac{3}{16} |\psi|^4 \psi = 0. \quad (6.13)$$

We note that the negative imaginary coefficient of the cubic term arises directly from the rescaling, though it can be mapped to the standard $+i$ form by a time reflection $T \rightarrow -T$.

The value $\beta = -3/16$ places the interaction-driven Carroll system in a specific stability regime. While the minimal coupling generates a repulsive (defocusing) quintic term, numerical analysis (Fig. 4) reveals that this does not lead to incoherent dispersion. Instead, the derivative cubic nonlinearity (which promotes soliton formation) is sufficient to maintain the wave packet’s coherence against dispersion. The result is the formation of robust, localized solitary waves that propagate with a preserved profile over long evolution distances.

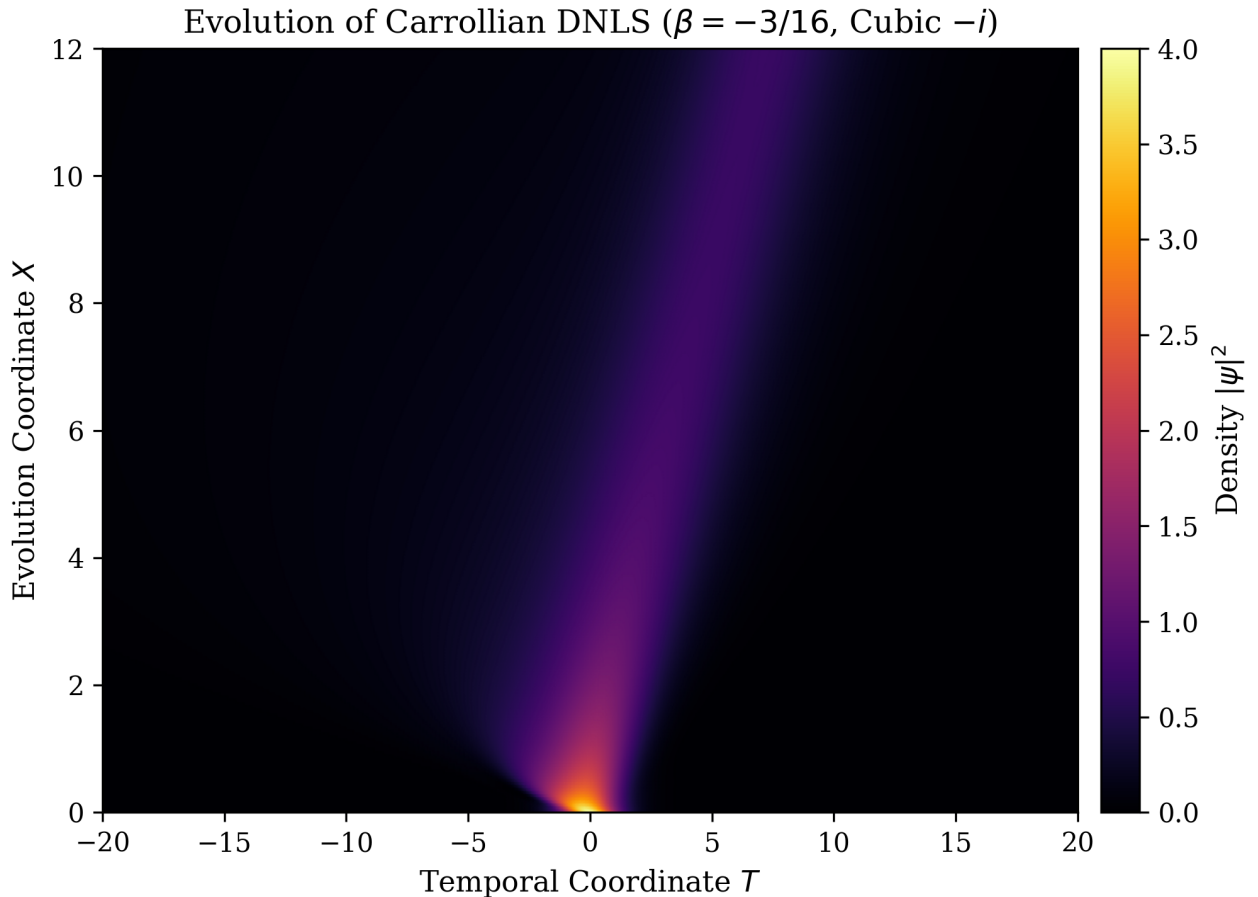


Figure 4: Numerical evolution of the interaction-driven Carroll gas density $|\psi(X, T)|^2$ for the derived parameters (cubic $-i$, quintic $\beta = -3/16$). The simulation demonstrates that the pulse remains strictly localized as it evolves along X . The dynamics are governed by the interplay between the derivative nonlinearity, which sustains the solitary wave structure, and the repulsive quintic term, which saturates the amplitude and ensures stability against collapse.

7 Carrollian Hohenberg–Kohn mapping and Kohn–Sham scheme

We motivate the density–current functional framework by minimally coupling the canonical pairs (x, P) and (t_i, E_i) to external Abelian gauge fields on equal- x slices. The momentum conjugate to x couples to a scalar field $\Phi(t)$ via

$$P \longrightarrow P - \frac{1}{c} \Phi(t), \quad (7.1)$$

while the temporal pairs couple to a gauge field $U(t)$ and internal interactions via

$$E_i \longrightarrow E_i - U(t_i) - \Omega_i^{\text{int}}(\mathbf{t}). \quad (7.2)$$

The resulting many-body Carroll generator is

$$\mathcal{H}_{\text{in}}^{(N)}[\Phi, U] = \sum_{i=1}^N \frac{1}{2mc^2} \left(\hat{E}_i - \Omega_i^{\text{int}}(\mathbf{t}) - U(t_i) \right)^2 + \sum_{i=1}^N \Phi(t_i), \quad \hat{E}_i = -i\hbar \partial_{t_i}, \quad (7.3)$$

where Ω_i^{int} encodes fixed internal interactions. Under the substitutions

$$q \leftrightarrow t, \quad \hat{p} \leftrightarrow \widehat{E}/c, \quad v(q) \leftrightarrow \Phi(t), \quad A(q) \leftrightarrow U(t), \quad (7.4)$$

where q is a 1D spatial coordinate, this problem is formally isomorphic to standard *one-dimensional* current-density functional theory (CDFT) [19–22]. As in 1D CDFT, $U(t)$ is defined only up to gauge transformations $U \rightarrow U + \partial_t \chi$ accompanied by $\Psi \rightarrow e^{\frac{i}{\hbar} \sum_i \chi(t_i)} \Psi$, while $\Phi(t)$ remains gauge invariant.

We import the existence and uniqueness theorems of CDFT without rederivation, assuming the Hamiltonian is bounded from below, the ground state is nondegenerate up to gauge, and v -representability holds. Thus, for fixed Ω_i^{int} , there exists a universal functional $F[n, j_t]$ of the temporal density $n(t)$ and physical current $j_t(t)$. Universality implies independence from (Φ, U) , though F depends parametrically on the internal interaction.

The interacting densities are reproduced by a fictitious noninteracting system via one-time orbitals $\{\varphi_k(t)\}$ solving the Carroll–Kohn–Sham equations

$$\frac{1}{2mc^2} \left(-i\hbar\partial_t - U_s[n, j_t] \right)^2 \varphi_k + \Phi_s[n, j_t] \varphi_k = \epsilon_k \varphi_k, \quad (7.5)$$

with

$$n(t) = \sum_k f_k |\varphi_k|^2, \quad j_t(t) = \frac{1}{mc^2} \sum_k f_k \text{Re}\{ \varphi_k^* (-i\hbar\partial_t - U_s) \varphi_k \}. \quad (7.6)$$

The effective fields Φ_s and U_s include external, Hartree, and exchange–correlation contributions determined by the functional derivatives of $F[n, j_t]$. This framework enables the analysis of collective temporal behavior and emergent many-body phenomena using the established language of spatial DFT.

8 Discussion

In this work we developed a many-body Carroll–Schrödinger framework in which the spatial variable x acts as an evolution parameter and the temporal variables $\mathbf{t} = (t_1, \dots, t_N)$ play the role of configuration coordinates. Starting from a relativistic multi-time Klein–Gordon model and performing a Carrollian contraction, we obtained a consistent equal- x generator that is a sum of temporal energy operators acting on $L^2(\mathbb{R}_t^N)$. Temporal interactions were introduced via minimal coupling, and an x -dependent gauge transformation mapped these couplings to explicit many-body potentials in the time variables, providing a systematic route to construct Carrollian partners of familiar Schrödinger models.

The analysis of spatial potentials revealed a characteristic Carrollian kinematics. When the starting point is a static spatial potential $U_{\text{tot}}(\mathbf{x})$, the transformed CS evolution depends on U_{tot} only through the net collective force $\sum_j \partial_{x_j} U_{\text{tot}}(\mathbf{x})$. For coupled harmonic oscillators this produces a calculable linear-in- t drive of the collective coordinate and explicit Gaussian N -body solutions. For any spatially translation-invariant interaction (including regularized one-dimensional Coulomb potentials), the internal forces cancel in the collective direction, so that the collective Carrollian dynamics becomes free and the potential reappears only through phases and boundary data. From the spatial viewpoint this yields a class of spatially homogeneous, boundary-data–determined evolutions without time-translation symmetry, reminiscent of homogeneous fluids whose dynamics is entirely fixed by their initial conditions and a global time-dependent drive. In this sense the construction

illustrates, in a simple many-body setting, how Carrollian ultralocality enforces consistency of spatially driven systems with their initial data.

On the operator side, we generalized the single-particle coordinate duality between the time-independent Schrödinger equation and a space-independent CS equation to separable many-body systems using Schwarzian relations for the inverse coordinate maps. For each particle a reparametrization $x_i = \delta_i(t_i)$ relates static Schrödinger potentials $V_{\text{sch}}^{(i)}(x_i)$ to one-body Carroll potentials $V_{\text{car}}^{(i)}(t_i)$ acting on the temporal coordinates. We also explored this Schwarzian map in an interacting setting, namely two coupled Schrödinger oscillators, which suggests that certain classes of separable interacting models can be transplanted into the Carrollian framework. Exchange symmetry was formulated directly in the time domain, leading to bosonic and fermionic sectors characterized by temporal bunching or antibunching through the second-order coherence function $g^{(2)}(t, t')$ on equal- x slices.

In a second-quantized description on equal- x slices, a two-time interaction kernel leads, in a short-memory limit analogous to the contact-interaction regime of the Lieb–Liniger gas, to a structure similar to a temporal derivative cubic–quintic nonlinear Schrödinger equation. In this limit the structure of the minimal coupling fixes the quintic coefficient to $\beta = -3/16$, placing the interaction-driven temporal Carroll gas in a specific universality class of derivative nonlinear Schrödinger systems. This provides a concrete example where Carrollian kinematics constrains the effective nonlinear dynamics of a many-body system in the time domain.

Finally, we identified a natural mapping between the static CS many-body problem and one-dimensional current-density functional theory (CDFT). By minimally coupling the canonical momentum P to a scalar field $\Phi(t)$ and the temporal energy E to a gauge field $U(t)$, the ground-state problem on equal- x slices can be written in a form that is formally isomorphic to one-dimensional CDFT. Rather than proving new existence theorems, we use this isomorphism to motivate a universal functional $F[n, j_t]$ of the temporal density $n(t)$ and temporal current $j_t(t)$ and to outline a Carrollian Kohn–Sham scheme in terms of one-time orbitals that reproduce (n, j_t) on equal- x slices.

The present analysis, while opening the door to multiparticle Carrollian quantum mechanics, is necessarily restricted. We have worked in 1+1 dimensions, considered spinless particles and specific classes of temporal and spatial potentials, and focused our explicit solutions on Gaussian states and exactly solvable models (such as coupled oscillators and the trivialized Coulomb gas). The coordinate duality was implemented for separable Schrödinger potentials and explored in an interacting example of two coupled harmonic oscillators; extending it to general N -body interacting static potentials would require genuine multivariable generalizations of the Schwarzian map and remains an open problem. Likewise, our discussion of Carrollian density-functional theory has been kept at a formal level: concrete temporal exchange–correlation approximations were not attempted here and would have to be adapted from the CDFT literature or reformulated to take into account the temporal behaviour of Carrollian particles.

Despite these limitations, the results illustrate that many-body Carroll–Schrödinger dynamics, coordinate dualities, temporal coherence and functional descriptions can be organized within a common framework. Beyond the intrinsic interest of Carrollian quantum systems, there are several potential areas of application. Carroll symmetry has already appeared in cosmology and dark-energy model building, where Carrollian fluids naturally realize an equation of state $\mathcal{E} + P = 0$ and provide a useful language for inflation and de Sitter-like phases [10, 11]. In parallel, Carrollian geometry and hydrodynamics have been linked to effective descriptions of strongly driven or constrained systems, including

Carrollian fluids and Bjorken flow, and other condensed-matter models with restricted mobility [36–38]. The spatially driven multiparticle Carroll systems studied here, with their homogeneous collective response and strong dependence on boundary data, may provide simple toy models for such homogeneous yet nonstationary Carrollian media.

A natural next step is to generalize the present construction to higher spatial dimensions and to more elaborate Carrollian field theories. The Carroll–Schrödinger equation itself admits higher-dimensional and gauge-coupled versions, both as the ultra-relativistic limit of tachyonic models and as field theories with nontrivial Carroll–Schrödinger symmetry algebras [3]. At the same time, two-time formulations of Carroll particles suggest that additional temporal and spatial dimensions can be incorporated within a unified constrained Hamiltonian framework [34]. Extending the many-body CS formalism along these lines, and combining it with temporal density functionals and DNLS-type effective theories, may open a bridge between Carrollian quantum mechanics, condensed-matter models with emergent Carroll symmetry, and cosmological applications such as dark energy dynamics.

References

- [1] J.-M. Lévy-Leblond, “Une nouvelle limite non relativiste du groupe de Poincaré,” *Ann. Inst. Henri Poincaré A* **3**, 1–12 (1965).
- [2] M. Najafizadeh, “Post-Carrollian mechanics, ideal gas, and gravity,” *Int. J. Mod. Phys. A* **40**, 2550122 (2025).
- [3] M. Najafizadeh, “Carroll–Schrödinger equation as the ultra-relativistic limit of the tachyon equation,” *Sci. Rep.* **15**, 13884 (2025).
- [4] J. Rojas, M. Arias and E. Casanova, “On the Schrödinger and Carroll–Schrödinger Equations: Dualities and Applications,” arXiv:2502.04562 [quant-ph] (2025).
- [5] P. A. M. Dirac, “Relativistic quantum mechanics,” *Proc. R. Soc. Lond. A* **136**, 453–464 (1932).
- [6] M. Lienert, S. Petrat and R. Tumulka, “Multi-time wave functions,” *J. Phys. A: Math. Theor.* **50**, 335301 (2017).
- [7] S. Petrat and R. Tumulka, “Multi-time Schrödinger equations cannot contain interaction potentials,” *J. Math. Phys.* **55**, 032302 (2014).
- [8] L. P. Horwitz, “Time and the evolution of states in relativistic classical and quantum mechanics,” arXiv:hep-ph/9606330 (1996).
- [9] L. P. Horwitz, *Relativistic Quantum Mechanics*, Fundamental Theories of Physics, Vol. 180 (Springer, Dordrecht, 2015).
- [10] J. de Boer, J. Hartong, N. A. Obers, W. Sybesma and S. Vandoren, “Carroll symmetry, dark energy and inflation,” *Front. Phys.* **10**, 810405 (2022).
- [11] J. de Boer, J. Hartong, N. A. Obers, W. Sybesma and S. Vandoren, “Carroll Stories,” *J. High Energy Phys.* **09**, 027 (2023).
- [12] R. Hanbury Brown and R. Q. Twiss, “A test of a new type of stellar interferometer on Sirius,” *Nature* **178**, 1046–1048 (1956).

- [13] L. Mandel and E. Wolf, *Optical Coherence and Quantum Optics* (Cambridge University Press, Cambridge, 1995).
- [14] E. H. Lieb and W. Liniger, “Exact analysis of an interacting Bose gas. I. The general solution and the ground state,” *Phys. Rev.* **130**, 1605–1616 (1963).
- [15] E. H. Lieb, “Exact analysis of an interacting Bose gas. II. The excitation spectrum,” *Phys. Rev.* **130**, 1616–1624 (1963).
- [16] K. Mio, T. Ogino, K. Minami and S. Takeda, “Modified nonlinear Schrödinger equation for Alfvén waves propagating along the magnetic field,” *J. Phys. Soc. Jpn.* **41**, 265–271 (1976).
- [17] D. J. Kaup and A. C. Newell, “An exact solution for a derivative nonlinear Schrödinger equation,” *J. Math. Phys.* **19**, 798–801 (1978).
- [18] G. P. Agrawal, *Nonlinear Fiber Optics*, 6th ed. (Academic Press, San Diego, 2019).
- [19] E. H. Lieb, “Density functionals for Coulomb systems,” *Int. J. Quantum Chem.* **24**, 243–277 (1983).
- [20] G. Vignale and M. Rasolt, “Density-functional theory in strong magnetic fields,” *Phys. Rev. Lett.* **59**, 2360–2363 (1987).
- [21] G. Vignale and M. Rasolt, “Current-density functional theory of electronic systems,” *Phys. Rev. B* **37**, 10685–10696 (1988).
- [22] E. Engel and R. M. Dreizler, *Density Functional Theory: An Advanced Course* (Springer, Berlin, 2011).
- [23] P. Hohenberg and W. Kohn, “Inhomogeneous electron gas,” *Phys. Rev.* **136**, B864–B871 (1964).
- [24] W. Kohn and L. J. Sham, “Self-consistent equations including exchange and correlation effects,” *Phys. Rev.* **140**, A1133–A1138 (1965).
- [25] N. D. Sen Gupta, “On an analogue of the Galilei group,” *Il Nuovo Cimento A* **44**, 512–517 (1966).
- [26] H. Bacry and J.-M. Lévy-Leblond, “Possible kinematics,” *J. Math. Phys.* **9**, 1605–1614 (1968).
- [27] C. Duval, G. W. Gibbons and P. A. Horvathy, “Conformal Carroll groups and BMS symmetry,” *Class. Quantum Grav.* **31**, 092001 (2014).
- [28] C. Duval, G. W. Gibbons and P. A. Horvathy, “Conformal Carroll groups,” *J. Phys. A: Math. Theor.* **47**, 335204 (2014).
- [29] A. Bagchi, A. Banerjee, R. Basu, S. Dutta and P. Sharma, “Carroll covariant scalar fields and flat holography,” *J. High Energy Phys.* **04**, 229 (2023).
- [30] C. Duval, P. A. Horvathy and L. Palla, “Carroll symmetry of plane waves,” *Ann. Phys. (N.Y.)* **442**, 168901 (2022).

- [31] M. Reed and B. Simon, *Methods of Modern Mathematical Physics, Vol. II: Fourier Analysis, Self-Adjointness* (Academic Press, New York, 1975).
- [32] D. Rivera-Betancour and M. Vilatte, “Revisiting the Carrollian scalar field,” *Phys. Rev. D* **106**, 085004 (2022).
- [33] K. Banerjee, S. Dutta and S. Mondal, “One-loop quantum effects in Carroll scalars,” *Phys. Rev. D* **108**, 085022 (2023).
- [34] A. Kamenshchik and F. Muscolino, “Looking for Carroll particles in two time space-time,” *Phys. Rev. D* **109**, 025005 (2024).
- [35] E. Bergshoeff, J. Gomis and G. Longhi, “Dynamics of Carroll particles,” *Class. Quantum Grav.* **31**, 205009 (2014).
- [36] A. Bagchi, K. S. Kolekar and A. Shukla, “Carrollian Origins of Bjorken Flow,” *Phys. Rev. Lett.* **130**, 241601 (2023), arXiv:2302.03053 [hep-th].
- [37] J. Armas and E. Have, “Carrollian Fluids and Spontaneous Breaking of Boost Symmetry,” *Phys. Rev. Lett.* **132**, 161606 (2024), arXiv:2308.10594 [hep-th].
- [38] L. Marsot, P. M. Zhang, M. Chernodub and P. A. Horvathy, “Hall Motions in Carroll Dynamics,” *Phys. Rept.* **1028**, 1–60 (2023), arXiv:2212.02360 [hep-th].